

RIGA TECHNICAL UNIVERSITY
Faculty of Transport and Mechanical Engineering
Institute of Biomedical Engineering and Nanotechnologies

Marina ROMANOVA

Doctoral Candidate of Doctoral study programme „Engineering Technology, Mechanics and Mechanical Engineering” (RMDM8), direction „Medical Engineering and Medical Physics”

**METHOD OF DOSIMETRY OF IONIZING RADIATION
BASED ON ELECTRON EMISSION FROM $ZrO_2:PbS$
NANOSTRUCTURED FILMS**

Summary of Doctoral Thesis

Field: Mechanical engineering
Subfield: Measuring instruments and metrology

Research supervisor
Dr.habil.phys., Professor
Yu. DEKHTYAR

Riga 2015

UDK 614.876(043.2)
Ro 413 m

Romanova M. Method of dosimetry of ionizing radiation based on electron emission from $ZrO_2:PbS$ nanostructured films. Summary of Doctoral Thesis.- R.:RTU, 2015.-36 p.

Printed according to the decision of RTU BINI from January 22, 2015, the Protocol No.3



This work has been supported by the European Social Fund within the projects «Support for the implementation of doctoral studies at Riga Technical University» No. 2009/0144/1DP/1.1.2.1.2/09/IPIA/VIAA/005, and « Support for the implementation of doctoral studies at Riga Technical University – 2», No. 2011/0053/1DP/1.1.2.1.2/11/IPIA/VIAA/003

**DOCTORAL THESIS
SUBMITTED FOR THE DEGREE OF DOCTOR OF ENGINEERING
SCIENCES
AT RIGA TECHNICAL UNIVERSITY**

The doctoral thesis submitted for the degree of Doctor of Engineering Sciences will be defended at the public session of Promotion Council „RTU P-16”, Riga Technical university, on June 30th, 2015, Faculty of Transport and Mechanical Engineering, Ezermalas Street 6a, room 405, at 13:00.

OFFICIAL REVIEWERS

Professor, Dr.phys. Jānis Kalnačs
Institute of Physical Energetics, Latvia

Leading researcher, Dr.habil.phys. Donāts Millers
Institute of Solid State Physics, University of Latvia, Latvia

Professor, Dr.phys. Diana Adliene
Kaunas University of Technology, Lithuania

CONFIRMATION

I hereby confirm that I have written this doctoral thesis that has been submitted for assessment at Riga Technical University for the degree of Doctor of Engineering Sciences. The doctoral thesis has not been submitted for the doctorate degree at any other higher educational institution.

Marina Romanova(Signature)

Date:

The doctoral thesis is written in Latvian, contains introduction, 3 chapters, conclusions, recommendations, list of literature, 75 pages in total. The list of literature contains 74 titles.

CONTENTS

GENERAL DESCRIPTION OF DOCTORAL THESIS	5
Thesis topic rationale	5
Purpose and tasks of the thesis	5
Research methods.....	6
Theses to defend.....	6
Scientific novelty	6
Practical significance	6
Approbation of the thesis	7
Publications	8
1. REVIEW OF LITERATURE	10
1.1. Nanodosimetry	10
1.2. Detectors in nanodosimetry.....	10
2. EXPERIMENTAL PART	12
2.1. Preconditions for the development of nanodosimeter.....	12
2.1.1. Physical basis of nanodosimeter	12
2.1.2. Dose readout.....	13
2.2. Samples and research methods.....	13
2.2.1. ZrO ₂ :PbS nanostructured films for nanodosimetry.....	13
2.2.2. Characterization of ZrO ₂ :PbS nanostructured films	15
2.2.3. Photoelectron emission as a method of dose readout.....	15
2.2.4. Types of radiation for dose delivery	16
2.2.5. Annealing of ZrO ₂ :PbS nanostructured films	17
3. RESULTS AND DISCUSSION	17
3.1. Theoretical justification for the use of nanoparticles in nanodosimetry	17
3.2. Practical realization of the nanodosimeter	19
3.3. General processing of photoelectron emission spectra	20
3.4. Influence of PbS nanoparticles on photoelectron emission of ZrO ₂ :PbS nanostructured films	21
3.5. Influence of radiation on photoelectron emission of ZrO ₂ :PbS nanostructured films.....	25
3.5.1. Influence of non-ionizing ultraviolet radiation on photoelectron emission of ZrO ₂ :PbS nanostructured films	25
3.5.2. Influence of ionizing electron beam radiation on photoelectron emission of ZrO ₂ :PbS nanostructured films	26
3.5.3. Electron beam radiation dose measurement error	27
3.6. Restoration of ZrO ₂ :PbS nanostructured films after exposure to electron beam radiation.....	28
3.6.1. Selection of annealing temperature	28
3.6.2. Time-dependent changes of photoemission spectra after annealing	29
3.6.3. Exposure of ZrO ₂ :PbS nanostructured films to electron beam radiation after annealing	30
CONCLUSIONS	32
RECOMMENDATIONS	32
LIST OF LITERATURE	33
ACKNOWLEDGEMENTS	36

GENERAL DESCRIPTION OF DOCTORAL THESIS

Thesis topic rationale

Cancer is the second leading cause of death in the EU Member States after cardiovascular diseases; moreover, the mortality rates in Latvia, Lithuania and Estonia are among the highest in Europe [36]. In 2014, cancer was the cause of death in 21% of cases in Latvia [47]. One of the main methods of cancer treatment is radiation therapy [6]. In Latvia, at least 20% of all oncology patients receive radiotherapy as a sole treatment or in combination with other treatments [46].

During radiotherapy, malignant tumor is irradiated with ionizing radiation. The radiation breaks the chemical bonds of DNA molecules of cancer cells, as the result the cells can no longer divide and die [22]. However, in the same way radiation affects DNA molecules of healthy tissue. Therefore, it is important to increase the accuracy of radiation delivery to cancer tissue in order to reduce the dose of radiation absorbed by the surrounding healthy tissue. To ensure this, it is important to control the area where radiation is delivered and the value of absorbed radiation dose which can be measured with dosimeters.

Taking into account the effects of radiation on DNA molecule having a diameter of 2 nm, it is important to know the value of radiation dose absorbed by a nano-sized biological object. Currently, there are no dosimeters which are capable of measuring the dose absorbed in nano objects having size similar to DNA molecule, therefore the value of absorbed dose is simulated, e.g. using Monte Carlo methods [39, 53]. In order to measure the radiation dose absorbed by nano-objects and thus to verify and refine simulation results, it is necessary to design a nanodosimeter and develop a method of its usage.

Method of dosimetry of ionizing radiation which allows to measure dose of radiation absorbed in objects having nano dimensions has been developed in the doctoral thesis. Lead sulphide (PbS) nanoparticles that are embedded in a dielectric nanofilm of zirconium oxide (ZrO_2 :PbS nanostructured film) were studied. Photoelectron emission (PE) spectroscopy has been used to read the dose of radiation absorbed in the films [26]. It has been also demonstrated in the thesis that it is possible to erase dose of radiation stored in ZrO_2 :PbS nanostructured films by performing annealing of the films.

Purpose and tasks of the thesis

Development of the method of dosimetry of ionizing radiation which allows to measure dose of radiation absorbed in objects with nano dimensions.

To achieve the purpose of the thesis the following tasks have been put forward:

- 1) To establish the theoretical basis for development of a nanodosimeter.
- 2) To offer a practical realization of the nanodosimeter that will be used for further experiments.
- 3) To develop a method of reading the signal from the nanodosimeter.
- 4) To develop a calibration curve that establishes relation between the signal of the nanodosimeter and the absorbed dose of radiation. To estimate the error of dose measurement using the developed calibration curve.
- 5) To develop a restoration method of dosimetric properties of the nanodosimeter after irradiation.
- 6) To develop recommendations for application of the nanodosimeter in nanodosimetry.

Research methods

ZrO₂:PbS nanostructured films were ordered and fabricated by sol-gel technique in Hebrew University of Jerusalem (Israel), Institute of Inorganic Chemistry, by the scientific group of Prof. Renata Reisfeld. To measure the thickness of the ZrO₂:PbS films and diameters of PbS nanoparticles scanning electron microscopy (FE-SEM Hitachi S4800 [24]) and etching with Ar⁺ ions (Gatan Inc. Precision Etching Coating System, Model 682 [20]) were used. PE current was registered using threshold photoelectron emission spectrometry. In order to deliver dose of radiation, ZrO₂:PbS nanostructured films were exposed to ultraviolet (UV) radiation (HAMAMATSU Lightningcure LC5 L8222 UV source with 200 W gas discharge lamp L8251 [30, 51]) and ionizing electron beam radiation (medical linear accelerator VARIAN CLINAC 2100CD [11]).

Theses to defend

- 1) *The method of extraction of PE signal associated with the presence of PbS nanoparticles out of PE spectra of ZrO₂:PbS nanostructured film.* Increment of PE current of ZrO₂:PbS film calculated in a photon energy range from 4,9 to 5,5 eV is associated with the presence of PbS nanoparticles in ZrO₂ film. PE current increases with increase in mole percent of PbS in ZrO₂ film.
- 2) *The method of dosimetry of ionizing radiation based on PE from ZrO₂:PbS nanostructured film (the nanodosimeter).* Absorbed dose of radiation influences increment of PE current calculated in a photon energy range from 4,9 to 5,5 eV. In order to determine dose of radiation absorbed in ZrO₂:PbS nanodosimeter, change of the increment of PE current after irradiation has to be compared with the calibration curve of the nanodosimeter.
- 3) *The method of restoration of dosimetric properties of the nanodosimeter made of ZrO₂:PbS nanostructured film after irradiation.* The nanodosimeter can be reused after its annealing in vacuum at 150 °C and it is possible to reuse the dosimeter not earlier than in 4 days after the annealing.

Scientific novelty

For the first time:

- 1) The possibility to create a nanodosimeter using nanoparticles as radiation-sensitive elements and PE as a method of absorbed dose readout has been demonstrated using ZrO₂:PbS nanostructured film as an example.
- 2) The PE signal associated with the presence of PbS nanoparticles was extracted out of PE spectra of ZrO₂:PbS nanostructured films.
- 3) The method of dosimetry of ionizing radiation has been developed that allows to measure dose of ionizing radiation absorbed in ZrO₂:PbS nanostructured films (demonstrated by the example of 9 MeV electron beam radiation in the dose range of 0–10 Gy).
- 4) The method of annealing of irradiated ZrO₂:PbS nanostructured films was developed and demonstrated which erases dose of radiation stored in the films and restores dosimetric properties of the films.

Practical significance

The developed method of dosimetry will promote the development of nanodosimeters based on radiation sensitive nanostructures. The use of nanodosimeters in radiobiology will result in deeper understanding of the effects of radiation on biological nanoobjects. This in turn will increase efficiency and safety of radiation therapy.

Approbation of the thesis

The results of the thesis were presented at the following scientific conferences:

- 1) 6th International Conference on Medical Physics "Medical Physics in the Baltic States 2008", October 10-11, 2008, Kaunas, Lithuania;
- 2) Riga Technical University 49th International Scientific Conference, October 13-15, 2008, Riga, Latvia;
- 3) The NATO Advanced Study Institute "Technological Innovations in Detection and Sensing of Chemical Biological Radiological Nuclear Threats and Ecological Terrorism", June 7-17, 2010, Chisinau, Moldova;
- 4) Riga Technical University 51th International Scientific Conference, October 11-15, 2010, Riga, Latvia;
- 5) 15th Nordic-Baltic Conference on Biomedical Engineering and Medical Physics (NBC 2011), June 14-16, 2011, Aalborg, Denmark;
- 6) International Conference "Functional Materials and Nanotechnologies" (FM&NT-2011), April 5-8, 2011, Riga, Latvia;
- 7) 3rd Joint World Congress of Latvian Scientists and 4th Congress of Letonika: section "Technical Sciences", October 24-27, 2011, Riga, Latvia;
- 8) Biomedical Engineering 2011, October 27-28, Kaunas, Lithuania;
- 9) International Conference "Functional Materials and Nanotechnologies" (FM&NT-2012), April 17-20, 2012, Riga, Latvia;
- 10) 2nd International Conference on Nanotechnologies and Biomedical Engineering (ICNBME-2013), April 18-20, 2013, Chisinau, Moldova;
- 11) Science, Technology and Innovative Technologies in the Prosperous Epoch of the Powerful State, June 12-14, 2013, Ashgabat, Turkmenistan;
- 12) International Conference on Bionics and Prosthetics, Biomechanics and Mechanics, Mechatronics and Robotics (ICBBM 2013), June 17-21, 2013, Riga, Latvia;
- 13) 10th International Conference on Nanosciences & Nanotechnologies (NN13), July 9-12, 2013, Thessaloniki, Greece;
- 14) 15th International Conference-School "Advanced Materials and Technologies", August 27-31, 2013, Palanga, Lithuania;
- 15) Riga Technical University 54th International Scientific Conference, October 14-16, 2013, Riga, Latvia;
- 16) The 13th International Conference on Global Research and Education "Inter Academia 2014", September 10-12, 2014, Riga, Latvia.

The doctoral thesis continues the research of Institute of Biomedical Engineering and Nanotechnologies of RTU on application of $ZrO_2:PbS$ nanostructured films in the dosimetry of ionizing radiation started in 2008, the year when the author of the thesis defended her bachelor thesis entitled "Photoelectron Spectroscopy of PbS ZrO_2 nanofilms" (original title: *PbS ZrO_2 nanokārtnu fotoelektronu spektroskopija*). In 2009 the author defended master thesis entitled "Influence of Electron Radiation on Photoemission Spectra and Surface Electric Potential of $ZrO_2:PbS$ films" (original title: *Elektronu starojuma ietekme uz $ZrO_2:PbS$ plēvīšu fotoemisijas spektriem un virsmas elektrisko potenciālu*).

In the direction of the research the following bachelor theses were developed supervised by the author:

- Borzola, Aleksandra. *Penumbra formation in the $ZrO_2:PbS$ film covered by a mask and irradiated with UV radiation*. (Original title: *Pusēnas veidošanās pārklātajā ar masku $ZrO_2:PbS$ kārtiņā, apstarojot to ar ultravioleto starojumu*). Riga: [RTU], 2012. 51 p.

- Beļikovs, Vjačeslavs. *Elektronu un gamma starojuma ietekme uz ZrO₂:PbS filmas virsmas elektrisko potenciālu un pjezoatsauci*. Rīga: [RTU], 2012. 88 p.
- Krumpāne, Diāna. *Influence of electron and gamma radiation on photoemission properties of ZrO₂:PbS film*. (Original title: *Elektronu un gamma starojuma ietekme uz ZrO₂:PbS filmas fotoemisijas īpašībām*.) Rīga: [RTU], 2012. 52 p.
- Rešetņikova, Aļisa. *Influence of cleaning of ZrO₂:PbS nanolayer surface and annealing on photoemission*. (Original title: *ZrO₂:PbS nano pārklājuma virsmas attīrīšanas un atkvēlināšanas ietekme uz fotoemisiju*). Rīga: [RTU], 2013. 66 p.
- Kovaļovs, Pāvels. *Applicability of photoemission from ZrO₂:PbS film in nanodosimetry of gamma and electron radiation*. (Original title: *ZrO₂:PbS filmas fotoemisijas izmantošanas iespējamība gamma un elektronu starojuma nanodozimētrijai*.) Rīga: [RTU], 2013. 72 p.

Publications

The results of the thesis are published:

I. Chapter of multi-authored monograph

1) Dekhtyar Yu., Romanova M., Anischenko A., Sudnikovich A., Polyaka N., Reisfeld R., Saraidarov T., Polyakov B. PBS Nanodots for Ultraviolet Radiation Nanosensor. - Vaseashta A., Braman E., Susmann P., eds. *Technological Innovations in Sensing and Detection of Chemical, Biological, Radiological, Nuclear Threats and Ecological Terrorism*. - Dordrecht: Springer Science+Business Media B.V., 2012. - pp.361-366. ISBN 978-940072487-7 (**SCOPUS**)

2) Dekhtyar Yu., Krumpāne D., Perovicha K., Reisfeld R., Romanova M., Saraidarov T., Surkova I. Electron Emission Standed Nanodosimetry and Gas Detection. - Vaseashta A., Khudarverdyan S., eds. *Advanced Sensors for Safety and Security*. - Dordrecht: Springer Science+Business Media Dordrecht, 2013. - pp.173-180. ISBN 978-94-007-7002-7 (**SCOPUS**)

II. Publications in reviewed scientific journals

1) Dekhtyar Yu., Krumpāne D., Perovicha K., Reisfeld R., Romanova M., Saraidarov T., Soudnikovich A., Surkova I. Electron Emission for Nanodosimetry of Ionizing Radiation and Gas Sensing// *Chemical Sensors*. - 2013. - Vol.3. - Article ID6. - pp.1-4.

III. Proceedings of scientific conferences

1) Dekhtyar Yu., Kovalovs P., Krumpāne D., Reisfeld R., Resetnikova A., Romanova M., Saraidarov T., Surkova I. Photoelectron Emission from PbS Nanodots for Dosimetry of Ionizing Radiation// *Proceedings of the 9th Baltic - Bulgarian Conference on bionics and prosthetics, biomechanics and mechanics, mechatronics and robotics: ICBBM 2013, Latvia, Riga, 17-21 June, 2013*. Rīga: ICBBM Conference Committee, 2013. - pp.207-210.

2) Dekhtyar Yu., Polyaka N., Reisfeld R., Romanova M., Saraidarov T., Soudnikovich A. ZrO₂ Glass Films Influenced by Ultraviolet Radiation// *Medical Physics in the Baltic States 2008: Proceedings of the 6th International Conference on Medical Physics, Lithuania, Kaunas, 10-11 October, 2008*. - pp.27-31.

3) Dekhtyar Yu., Romanova M., Anischenko A., Sudnikovich A., Polyaka N., Reisfeld R., Saraidarov T., Polyakov B. PbS Nanodots For Ultraviolet Radiation Dosimetry// *IFMBE Proceedings*. - 2011. - Vol.34. - pp.133-136. (**SCOPUS**)

4) Dekhtyar Yu., Romanova M., Stalidzane K., Katashev A., Reisfeld R., Saraidarov T. PbS Nanodots for Electron Radiation Thin-Film Sensor// *Biomedical Engineering 2011: Proceedings of the International Conference, Lithuania, Kaunas, 27-28 October, 2011*. - pp.111-114.

5) Krumpāne D., Dekhtyar Yu., Surkova I., Romanova R. Photoelectron Emission as a Tool to Assess Dose of Electron Radiation Received by ZrO₂:PbS films// *2nd International*

Conference on Nanotechnologies and Biomedical Engineering (ICNBME-2013): Proceedings, Moldova, Chisinau, 18-20 April, 2013. Chisinau: Technical University of Moldova, 2013. - pp.649-651.

IV. Conference abstracts

1) Dehtjars J., Kataševs A., Romanova M., Stalidzāne K., Reisfeld R., Saraidarov T. ZrO₂ plānā kārtiņā ievietoto PbS nanodaļiņu pielietošana jonizējošā starojuma dozimetrijā// Apvienotais pasaules latviešu zinātnieku III kongress un Letonikas IV kongress: sekcija "Tehniskās zinātnes": tēžu krājums, Latvija, Rīga, 24.-27. oktobris, 2011. - 35. lpp.

2) Dekhtyar Yu., Anishchenko A., Polyakov B., Romanova M., Reisfeld R., Saraidarov T., Soudnikovich A. PbS Nanodots for Ultraviolet Radiation Nano Sensor// The NATO Advanced Study Institute, Technological Innovations in Detection and Sensing of Chemical Biological Radiological Nuclear Threats and Ecological Terrorism, Moldova, Chisinau, 7-17 June, 2010. - p.62.

3) Dekhtyar Yu., Katashev A., Reisfeld R., Romanova M., Saraidarov T., Stalidzane K. PbS Nanodots in ZrO₂ Thin-Film Matrix as a Possible Material for Microdosimetry of Ionizing Radiation// International Baltic Sea Region Conference "Functional Materials and Nanotechnologies 2012" (FM&NT): Proceedings, Latvia, Riga, 17-20 April, 2012. - p.87.

4) Dekhtyar Yu., Kovalovs P., Krumpāne D., Reisfeld R., Resetnikova A., Romanova M., Saraidarov T., Surkova I. Influence of Medical Electron Radiation and Annealing on Photoelectron Emission from Lead Sulphide Nanodots// Book of Abstracts of the 15th International Conference-School "Advanced Materials and Technologies", Lithuania, Palanga, 27-31 August, 2013. Kaunas: Technologija, 2013. - p.78.

5) Dekhtyar Yu., Perovicha K., Romanova M. Electron Emission Standed Nanodosimetry and Gas Detection// Advanced Research Workshop "Technological Innovations in CBRNE Sensing and Detection for Safety, Security, and Sustainability", Armenia, Yerevan, 29 Sep-1 Oct., 2012. Armenia: 2012. - p.53.

6) Dekhtyar Yu., Romanova M., Anischenko A., Sudnikovich A., Polyaka N., Reisfeld R., Saraidarov T., Polyakov B. Zirconia Films Doped with PbS Nanodots for Ultraviolet Radiation Dosimetry// International Baltic Sea Region Conference "Functional Materials and Nanotechnologies 2011" (FM&NT): Proceedings, Latvia, Riga, 5-8 April, 2011. - p.104.

7) Dekhtyar Yu., Kovalovs P., Reisfeld R., Rešetņikova A., Romanova M., Saraidarov T., Surkova I. PbS Nanodots for Nanodosimetry of Ionizing Radiation// The 13th International Conference on Global Research and Education, Inter-Academia 2014: Digest, Latvia, Riga, 10-12 September, 2014. Riga Technical University: 2014. - pp.178-179.

8) Krumpāne D., Dekhtyar Yu., Surkova I., Romanova M. Lead Sulfide Nanodots as a Tool for Detection of Dose of Electron Radiation Used in Radiation Therapy// "Science, Technology and Innovative Technologies in the Prosperous Epoch of the Powelful State". Abstracts of papers of the Intemational Scientific Conference, Turkmenistan, Ashgabat, 12-14 June, 2013. Academy of sciences of Turkmenistan: "Ylym" publishing house, 2013. - pp.342-345.

9) Romanova M., Krumpāne D., Reisfeld R., Saraidarov T., Surkova I., Dekhtyar Yu. Photoelectron Emission from PbS Nanodots for Dosimetry of Electron Radiation Used in Radiation Therapy// 10th International Conference on Nanosciences & Nanotechnologies (NN13): Abstract Book, Greece, Thessaloniki, 9-12 July, 2013. Thessaloniki: 2013. - p.297.

1. REVIEW OF LITERATURE

1.1. Nanodosimetry

Dosimetry of ionizing radiation is the field of engineering and applied physics that explores physical quantities characterizing the effects of ionizing radiation on biological and non-biological objects, as well as methods and tools for the measurement of these physical quantities.

Conventional dosimetry studies the absorption of radiation in objects with macro dimensions. The fundamental quantity in the traditional dosimetry is the absorbed dose (D) which is defined as energy (E) of ionizing radiation deposited per unit mass (m). In the SI system, the absorbed dose is measured in gray (Gy) [27, 32]:

$$D = E/m \text{ (Gy = J / kg)} \quad (1.1)$$

However, the irreversible damage to biological cells is mostly triggered by the ionizations produced in DNA molecule that has a diameter of 2 nm [22]. Consequently, there is a need to measure doses of radiation absorbed in biological targets with dimensions of few nanometers. Measurement of radiation absorption in nanometric targets is a task of *nanodosimetry*.

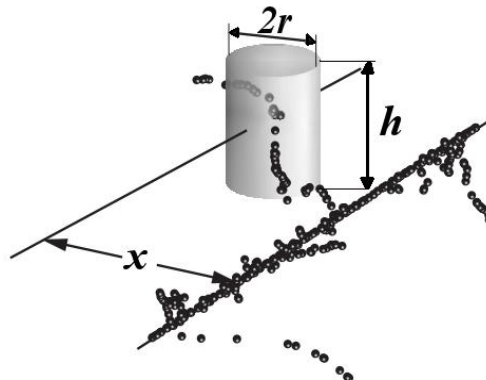


Fig. 1.1. Ionizations produced inside the cylindrical target having radius r and height h when ionizing particle is passing by at a distance x from the central axis of the cylinder [21]

Currently, it is not possible to measure dose of radiation absorbed in nanoobjects and the amount of the absorbed dose is estimated by computer simulations. It is possible to represent the shape of DNA molecule as a cylinder having radius r and height h (Fig. 1.1.) [21]. The ionizing particle is passing by at a distance x from the central axis of the cylinder and produces ionizations on its path. The absorbed dose results from the ionizations occurring inside the cylinder, therefore physical quantities in nanodosimetry take into account trajectory of ionizing particles in nanometric dimensions [21].

1.2. Detectors in nanodosimetry

Existing commercial dosimeters have a size of micrometers or millimeters (ionization microchambers, silicon diode array, scintillation dosimeters, diamond dosimeters, dosimetric films, transistors) [28, 31, 48, 52], therefore, it is not possible to apply them for nanodosimetry.

One of the methods to assess the dose absorbed in a nanovolume is to conduct physical modelling using gas dosimeters [5, 12, 13, 19]. A simplified diagram of the gas

dosimeter is shown in Fig. 1.2. Primary ionizing particle enters gas-filled chamber, produces ionizations in millimeter-sized wall-less cylindrical sensitive target and reaches the detector of primary radiation particles. The detector of primary radiation is synchronized with a counter of secondary ionizations. The counter is placed in vacuum and is capable of detecting single charged particles. When the primary particle hits the detector, the signal from the detector triggers the counter of secondary ionizations. Secondary electrons or ions are extracted from the chamber by applying appropriate polarity of electrical voltage and counted [34, 39]. The cylindrical shape of the sensitive target represents the shape of DNA molecule.

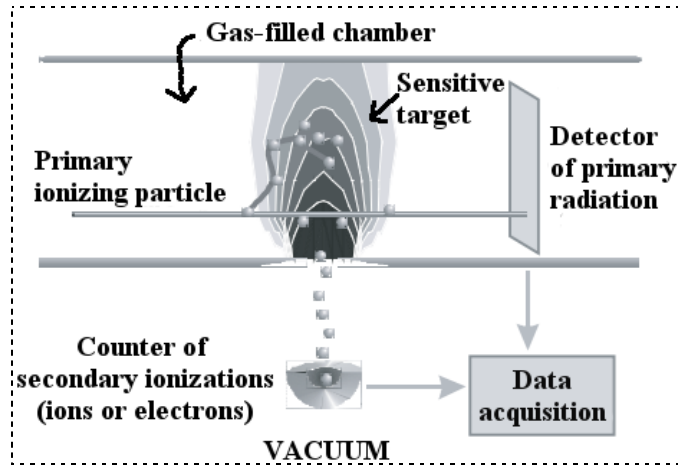


Fig. 1.2. A simplified diagram of the gas dosimeter [21]

DNA molecule has higher density than the gas inside the dosimeter. Therefore, density scaling is required to calculate the density of the gas applied for dose simulation [21]. Density scaling aims to link the number of ionizations measured in millimeter-sized gas target volumes with the number of ionizations expected in nano-sized DNA molecule.

Disadvantages of gas dosimeters are as follows:

- 1) Gas dosimeters do not provide direct dose measurements in nanovolumes. Dose absorbed in nanovolume is modelled by measurements in a millimetric sensitive target.
- 2) Gas dosimeters can only be used in real-time dosimetry because the ionizations in the gas disappear quickly after the radiation is turned off.
- 3) Gas dosimeters are not mobile due to the vacuum and gas supply systems.

The second approach to evaluation of the dose absorbed in nanovolume is based on application of luminescence.

Application of *X-ray luminescence* for nanodosimetry is described in Reference [49]. Nanoparticles of europium-doped yttrium oxide ($Y_2O_3:Eu$) with diameter of 150 nm exhibit red luminescence upon X-ray exposure. Linear correlation was observed between intensity of the main luminescence peak, area under luminescence spectra peaks and the maximal energy and current of X-ray. It was possible to visualize millimetric area in a silicone mouse phantom irradiated with X-ray using a conventional photo camera. However, it was not demonstrated whether it is possible to measure dose of radiation absorbed in nanovolume. Moreover, 150 nm diameter of $Y_2O_3:Eu$ nanoparticles exceeds several times 2 nm diameter of DNA molecule.

Potential application of *thermoluminescence* for nanodosimetry is described in Reference [17]. Thermoluminescent nanodosimetry is based on recombination of an electron with a hole in luminescent centres with dimensions comparable to DNA due to heating. Lithium fluoride doped with magnesium and titanium ($LiF:Mg,Ti$, commercial name TLD-100) was exposed to ionizing radiation and a glow curve of the material was recorded after the exposure. The glow curve was deconvoluted into single luminescence peaks and it was

found that one of the peaks results from recombination of electron and a hole within a trapping centre of 2 nm. Ratio of the peak intensity to the main peak intensity increased with increase in ionizing density of radiation and the authors hypothesize that this ratio can correlate with number of ionization produced in 2 nm large segment of DNA molecule.

2. EXPERIMENTAL PART

2.1. Preconditions for the development of nanodosimeter

2.1.1. Physical basis of nanodosimeter

Ionizing radiation generates free charge carriers (electrons) in the material of the dosimeter. Concentration of the free electrons will depend on the absorbed dose of radiation. The free electrons will move through conduction band until they are captured by electron traps which are localized states located within the band gap (Fig. 2.1). For dose measurements it is important to store the trapped charge for a long time, therefore, nanodosimeter must be made of dielectric or semiconductor material with a wide band gap. The opposite situation is also possible when the trapped electrons already exist in a material before the irradiation and ionizing radiation liberates these electrons. The liberated electrons will recombine with holes and concentration of the trapped electrons will be reduced.

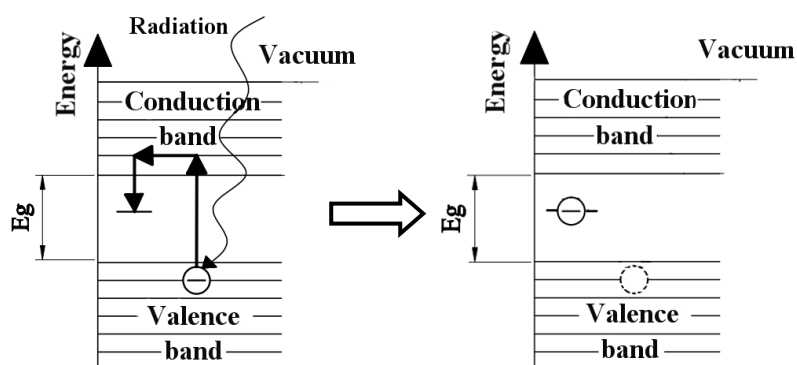


Fig. 2.1. Ionizing radiation excites an electron from valence band to conduction band, the electrons is travelling through the conduction band until it is trapped by localized states

In the thesis, radiation sensitive nanoparticles are proposed for active sensitive elements of the nanodosimeter. The diameter of the nanoparticles is of several nanometers which corresponds to the diameter of DNA molecule and therefore takes into account dose delivery mechanisms at nanoscale.

Nanoparticles must satisfy the following requirements:

- 1) In order to effectively absorb ionizing radiation, the nanoparticles must be made of material with high atomic number (Z number).
- 2) Decrease in the value of the absorbed dose accumulated in the nanodosimeter is not permitted in time interval between dose absorption and dose readout, therefore nanoparticles must be made of dielectric or semiconductor material with a wide band gap in order to store the trapped electric charge for a long time.
- 3) In order to ensure chemical and physical stability of nanoparticles, they must be embedded in a nanofilm:
 - a) the nanofilm must be resistant to external influences;
 - b) nanoparticles and nanofilm materials must be mutually inert.

2.1.2. Dose readout

It is possible to evaluate the absorbed dose of radiation by measuring the amount of charge trapped in localized states. The trapped electrons can be detected either by electrical contact or noncontact measurements. Any contact physically attached to a nanostructure will form interface with the nanostructure and influence results of measurements by increasing error of dose measurement. It is possible to measure the amount of the trapped electrons in a noncontact way by recording threshold FE current excited by UV photons having energy close to 4–6 eV photoelectric work function of the solids [15]. Photoelectric work function ϕ is the minimum photon energy required to liberate an electron from the solid (Fig. 2.2(a)). If the work function equals to 4–6 eV, the liberated electrons receive the kinetic energy of ≤ 4 –6 eV and they are emitted from the surface depth of 0,3–10 nm (Fig. 2.2(b)) [15, 26, 45]. This depth is comparable to the size of the studied nanoobjects (diameter of DNA molecule and diameter of nanoparticles).

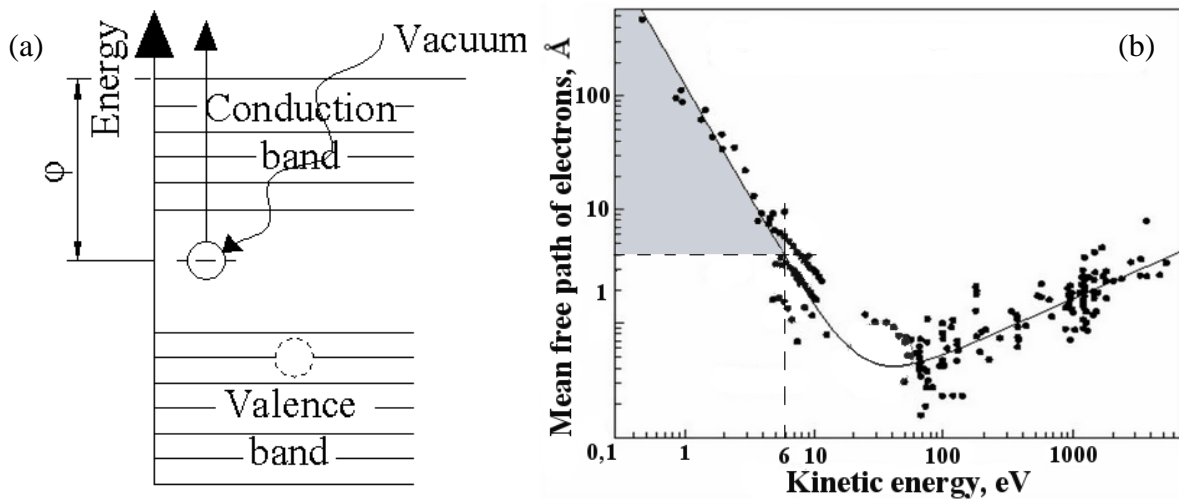


Fig. 2.2. Characteristics of photoelectron emission

(a) photoelectric work function; (b) mean free paths of electrons in solids depending on kinetic energy of the electrons [45]

Photoelectric work function equals to 4–6 eV for semiconductors [57]. This defines the material of the nanoparticles.

It is common for semiconductor nanoparticles to have surface defect states. Therefore, the nanoparticles used for detection of different kinds of radiation are enclosed in a passivating dielectric matrix with a wide band gap. The matrix preserves optical, electrical and chemical properties of the nanoparticles [2]. In addition, the dielectric matrix helps to preserve the electric charge induced in the nanoparticles under influence of ionizing radiation.

2.2. Samples and research methods

2.2.1. $\text{ZrO}_2\text{:PbS}$ nanostructured films for nanodosimetry

For nanodosimetry research $\text{ZrO}_2\text{:PbS}$ nanostructured films were used in the thesis with PbS nanoparticles acting as active elements. Lead is a material with a high atomic number ($Z = 82$) and is an effective absorber of ionizing radiation. PbS nanoparticles exhibit stable physical and chemical properties and are used in photonics for detection of solar

energy [29]. The technologies of stabilizing the surface of PbS nanoparticles by embedding them in a dielectric ZrO₂ matrix are developed [40].

ZrO₂:PbS nanostructured films were ordered and fabricated in Hebrew University of Jerusalem (Israel), Institute of Inorganic Chemistry, by the scientific group of Prof. Renata Reisfeld. The sol-gel technique was used for fabrication [42, 44]. ZrO₂:PbS films were deposited onto a glass substrate (1 mm thick microscope glass slides) (Fig. 2.3). The sol-gel technique has the following advantages: fabrication of samples at low temperatures, high degree of purity, homogeneity, nanoparticles can be fabricated at predetermined concentrations and with predefined diameters, there is no need to form chemical bonds between individual nanoparticles to hold them together [8].

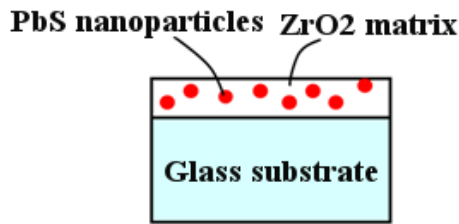


Fig. 2.3. Schematic representation of ZrO₂:PbS nanostructured films deposited on microscope glass slides

ZrO₂:PbS films were fabricated in the following steps, described in detail in [44]:

- 1) Preparation of ZrO₂ precursor solution.
- 2) Preparation of PbS precursor solution.
- 3) Preparation of ZrO₂:PbS solution from ZrO₂ and PbS precursor solutions.
- 4) Deposition of ZrO₂:PbS film onto microscope glass slide substrate. The glass substrate is immersed into ZrO₂:PbS solution and withdrawn at the rate of 20 cm/min. The deposition is performed at room temperature.
- 5) ZrO₂:PbS films are dried at 40 °C for one hour.
- 6) Annealing of ZrO₂:PbS films at 200 °C during 30 minutes.

The films were fabricated with PbS mole percent of 20% and 50%. Mole percent for PbS is calculated during preparation of ZrO₂:PbS solution (Step 3) with respect to total amount of moles of ZrO₂ + PbS constituents:

$$X_{PbS} = \frac{n_{PbS}}{n_{PbS} + n_{ZrO_2}} \cdot 100\% \quad (2.1)$$

where X – the mole percent of a constituent;

n – the amount of moles of a constituent.

Aggregation of PbS nanoparticles takes place when mole percent of PbS is 50% [42, 44]. The aggregated nanoparticles cannot be used for nanodosimetry, however, the films with such mole fraction were fabricated in order to identify PE properties inherent to PbS material. Increase in the mole percent of PbS results in larger PE signal of PbS in PE spectra of ZrO₂:PbS films.

In order to identify PE properties inherent to ZrO₂ material, ZrO₂ films without PbS nanoparticles were fabricated and deposited onto microscope glass slide substrate.

ZrO₂ matrix is an amorphous material with 5 eV wide band gap [16, 44]. The band gap of PbS nanoparticles depends on the diameter of the nanoparticles (Fig. 2.4) [42].

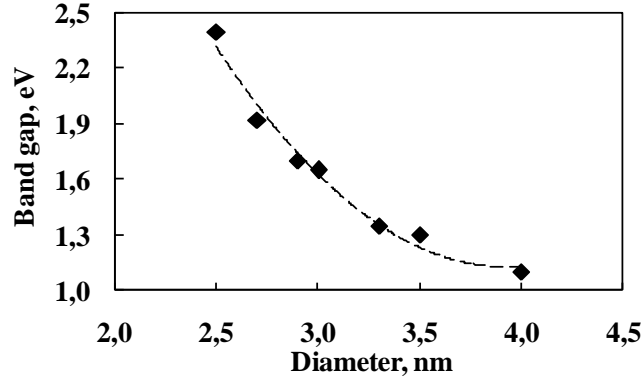


Fig. 2.4. Dependence of the band gap of PbS nanoparticles on their diameter [42]

Photoelectric work function φ (eV) equals to the sum of band gap E_g (eV) and electron affinity EA (eV) [58]:

$$\varphi = E_g + EA \quad (2.2)$$

$EA \approx 2.5$ eV for ZrO_2 material [41], EA is from 3.5 to 4.0 eV for PbS nanoparticles with size from 2.9 to 4.8 nm [25]. According to Equation (2.2) and Fig.2.4, $\varphi_{ZrO_2} \approx 7.5$ eV, $\varphi_{PbS} \approx 5.2$ eV. This means that it is possible to register PE from PbS nanoparticles using photon energies of 4–6 eV.

The fabricated samples were cut to a size of 25×10 mm using diamond glass cutter. To verify that the cutting process did not damage the surface of the samples, they were controlled visually using Motic BA400 optical microscope [33] with a magnification of 200 times.

After cutting, the samples were cleaned in ultrasonic bath *Bandelin Sonorex RK31* [54] during 10 minutes in a solution containing 96% ethanol and distilled water in a volume ratio of 1:2. After ultrasonic treatment, the samples were dried for 3-5 s with compressed nitrogen at room temperature.

2.2.2. Characterization of ZrO_2 :PbS nanostructured films

The thickness of ZrO_2 :PbS films deposited onto glass substrate and diameter of PbS nanoparticles were measured using SEM (scanning electron microscopy).

In order to discern PbS nanoparticles, the outer layer of ZrO_2 :PbS film was etched using Ar^+ ions before performing SEM measurements. Method of ion etching was chosen because it provides better purity of the surface of the samples compared to chemical etching or mechanical polishing. Energy of Ar^+ ions was 5 keV, current 300 mA.

2.2.3. Photoelectron emission as a method of dose readout

PE was measured in vacuum of 5×10^{-5} Torr at room temperature using photoelectron emission spectrometer [1] which provides photostimulation of the sample surface and registers the current of the emitted photoelectrons. Electronic system of the spectrometer [1] enables detection of single electrons.

PE was excited by 30 W deuterium arc lamp *DDS-30* that emits UV light of continuous spectra in a range of 186–360 nm [50, 56]. Wavelengths of 200–270 nm were used to excite PE. PE was not observed at wavelengths above 270 nm and the wavelengths below 200 nm were absorbed by atmospheric oxygen [9] (UV light travels the distance from the lamp till the entrance of vacuum chamber at atmospheric pressure).

PE data was recorded using personal computer with integrated emission counting module *Hamamatsu M8784* [37].

2.2.4. Types of radiation for dose delivery

2.2.4.1. Non-ionizing ultraviolet radiation

In order to obtain PE signal of $\text{ZrO}_2\text{:PbS}$ nanostructured films which is influenced by absorption of radiation, the films were irradiated with non-ionizing UV light and PE spectra of non-irradiated and irradiated films were compared.

UV radiation has higher absorption coefficient than ionizing radiation [38]. As a result of this, UV radiation influences absorption-dependent PE signal of $\text{ZrO}_2\text{:PbS}$ films more intensively than ionizing radiation. Therefore, UV radiation was used as a model for ionizing radiation in order to obtain absorption-dependent PE signal which to be used later in research with ionizing radiation.

Maximum intensity of *L8251* UV lamp is in the range of 300-400 nm [30]. Unlike the UV radiation of *DDS-30* lamp that was used to excite PE from $\text{ZrO}_2\text{:PbS}$ films, UV light of *L8251* lamp is non-ionizing, because PE from $\text{ZrO}_2\text{:PbS}$ films was not observed when the wavelengths exceed 270 nm (see 2.2.3. Chapter). However, transitions of electrons between localized states can happen under influence of non-ionizing UV.

Irradiation of the films was carried out at a distance of 40 cm between the output of the light guide and the surface of the films in order to avoid heating up the films. This distance was selected in experimental way by measuring temperature of the surface of the films using thermocouple. UV intensity at the distance of 40 cm was calculated from technical specifications of *L8222* lamp and was equal to 5 mW/cm^2 . Time of UV exposure varied from 5 to 75 minutes. Dose of radiation absorbed in the films was proportional to the time of UV exposure.

2.2.4.2. Ionizing electron beam radiation

$\text{ZrO}_2\text{:PbS}$ films were exposed to 9 MeV electrons in a dose range of 0–10 Gy. Dose rate was 3 Gy/min which is one of dose rates used for radiation therapy.

The films were positioned on the treatment table of linear accelerator at a distance $\text{SSD} = 100 \text{ cm}$ (SSD – source-skin distance means the distance from the radiation source to the exposed surface), radiation field size was $10 \times 10 \text{ cm}$. The selected parameters are standard parameters for dosimetric tests [14].

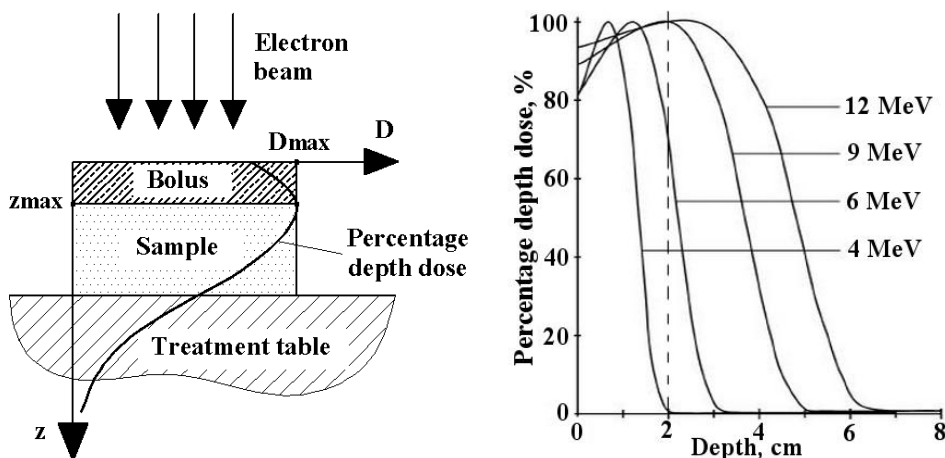


Fig. 2.5. Maximum dose delivery to the surface of the films
(a) applying a bolus; (b) percentage depth dose curve for electron beams with different energies [7]

Electrons deposit their maximum energy not precisely on the surface of the treated object but at a depth of z_{max} . For the maximum dose delivery exactly to the surface boluses are placed on the surface of the treated object – the plates of material with density equivalent to the biological tissue and having thickness of z_{max} (Fig. 2.5(a)).

The value of z_{max} depends on the energy of the electron beam (Fig. 2.5(b)). Boluses with thickness of 0,5 and 1 cm that can be placed on the top of each other were used for the irradiation. The energy of 9 MeV was chosen for the irradiation because in this case $z_{max} = 2$ cm and it was possible to select precisely the thicknesses of boluses.

2.2.5. Annealing of ZrO₂:PbS nanostructured films

Before exposing the dosimeter to radiation, it is necessary to remove the dose accumulated in the dosimeter after previous exposure times, i.e. to ensure that the dosimetric material returns to its initial pre-irradiation condition. This can be achieved by annealing the dosimeter. Temperature and time of annealing depend on dosimetric material [18].

In the situation when radiation excites electrons to localized levels (Fig. 2.1), thermal energy is supplied to the trapped electrons during annealing. As the result, the electrons are released from their traps and recombine with holes existing in the valence band. This restores the dosimetric material into the initial condition [35]. In the opposite situation, i.e. when radiation decreases concentration of the trapped electrons, the initial condition is restored by supplying these electrons with energy in order to excite them back to localized levels.

Annealing technique is used in thermoluminescent dosimeters to read and simultaneously to erase the dose absorbed in the dosimeters [18].

In the doctoral thesis applicability of annealing method to erase the dose of electron radiation stored in ZrO₂:PbS films was examined. Annealing of the films was performed in vacuum chamber of photoemission spectrometer at vacuum 5×10^{-5} Torr. Annealing in vacuum prevented oxidation of surface of the films.

Annealing process was controlled by temperature controller *Heat Wave Labs 101303-23* [23] of the spectrometer. The films were heated at a linear rate of 10 °C/min to ensure uniform heating of the surface and prevent formation of mechanical stresses. After annealing, the films were cooled to room temperature in a vacuum at their natural rate. The cooling rate was lower than the heating rate.

3. RESULTS AND DISCUSSION

3.1. Theoretical justification for the use of nanoparticles in nanodosimetry

If DNA molecule is modelled as a cylinder (Fig. 1.1), the absorbed dose is formed from ionization occurring inside the cylinder. In this case Equation (1.1) can be written as:

$$D = \frac{dE}{dm} = \frac{dE}{d(V \cdot \rho)} = \frac{dE}{d(\pi \cdot r^2 \cdot h \cdot \rho)}, \quad (3.1)$$

where V – volume of the cylinder, nm³;
 ρ – density of the cylinder, g/nm.

The absorbed dose depends on radius r of the irradiated target (Equation (3.1)) and distance x (Fig. 1.1). In this case two possible mechanisms of dose delivery are possible. If $x > r$, the ionizations inside the cylinder are produced by secondary electrons created by primary ionizing particle. If $x \leq r$, the ionizations inside the cylinder are produced due to the primary ionizing particle itself. Therefore, for correct measurements of the dose absorbed in a

nanoobject, size of the dosimeter has to be comparable with the nanoobject absorbing the dose. Such nano-sized dosimeter takes into account the dose delivery mechanisms.

The ionizing particles scattered by surface also contribute to the dose absorbed in a volume:

$$D = D_{vol} + D_{sur}, \quad (3.2)$$

where D_{vol} – the dose absorbed in a volume, Gy;

D_{sur} – the dose absorbed in a volume due to scattering of radiation by the surface, Gy.

D_{vol} is proportional to the target volume and D_{sur} is proportional to the target surface area:

$$D_{vol} \sim V; \quad V = \pi r^2 \cdot h \quad (3.3)$$

$$D_{sur} \sim S; \quad S = 2\pi r \cdot (h + r) \quad (3.4)$$

where S – surface area of the cylindrical target, nm^2 .

Contribution of the surface to the absorbed dose:

$$D_{sur}/D_{vol} \sim S/V, \quad (3.5)$$

$$\frac{S}{V} = \frac{2\pi r(h+r)}{\pi r^2 \cdot h} = \frac{2(h+r)}{rh} = \frac{2}{r} + \frac{2}{h} \quad (3.6)$$

According to Equations (3.5) and (3.6), if $r \rightarrow 0$, then $(D_{sur} / D_{vol}) \rightarrow \infty$. One can conclude that decrease of r results in significant increase of contribution of the scattered photons to the absorbed dose. Thus, it is not possible to use macro or micro-sized dosimeters in case of biological nanoobjects ($r \rightarrow 0$) and nano-sized dosimeters must be used instead.

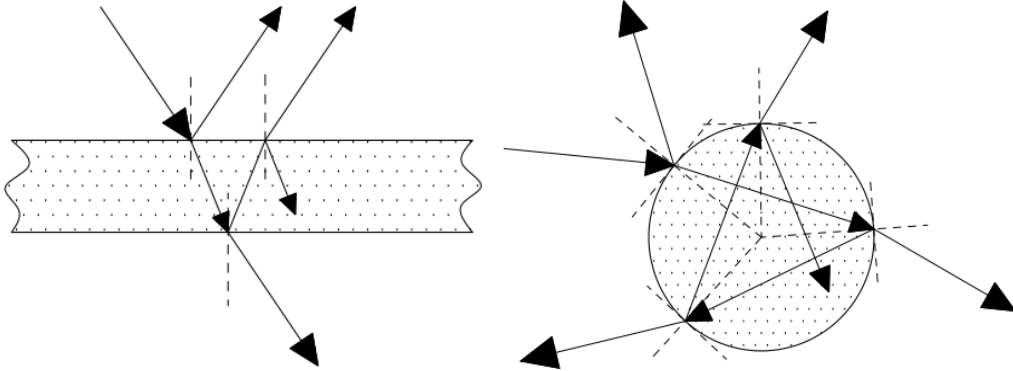


Fig. 3.1. The path of electromagnetic radiation in a flat object and a sphere

Dosimeters made of macro-sized material are used in conventional dosimetry. Fig. 3.1 shows comparison of path of electromagnetic radiation in a macro-sized object and in an object with dispersed nano-sized elements that can be represented by spheres. The dose absorbed in the spherical object is higher than the dose absorbed in the flat object due to multiple internal reflections from the walls of the sphere. What is more, reflections from the adjacent spheres also add to the absorbed dose. For that reason, the nanodosimeter must be made of nanoparticles in order to take into account dose delivery mechanisms at nanometric distances.

3.2. Practical realization of the nanodosimeter

Based on the theoretical justification of the use of nanoparticles and taking into account the information available in the literature, arrays of PbS nanoparticles embedded in ZrO_2 matrix were obtained which were further used for practical research of the nanodosimeter.

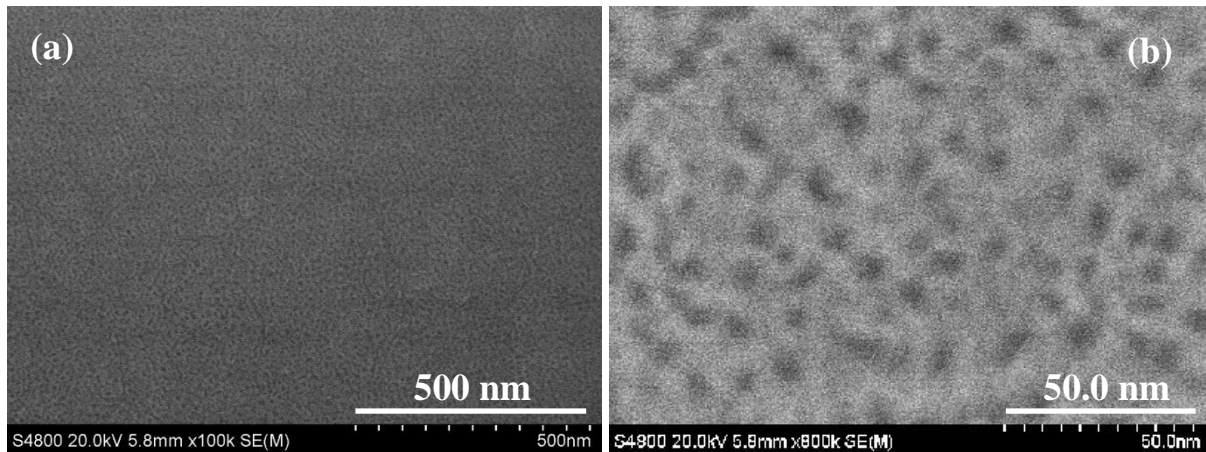
Thickness of fabricated ZrO_2 :PbS films was measured using SEM. The sample of ZrO_2 :PbS film on the glass substrate was cut in half with a diamond cutter and mounted vertically in the SEM sample holder with the cut edge at the top. The measured thickness of ZrO_2 :PbS films was 300 nm.

To analyse the diameters of PbS nanoparticles only the films with 20% mole percent of PbS were used (ZrO_2 :20%PbS) as aggregation of the nanoparticles takes place in the films with 50% mole percent of PbS making it impossible to distinguish between individual nanoparticles.

It was found during SEM analysis that PbS nanoparticles were not visible because they were covered with ZrO_2 matrix.

In order to liberate PbS nanoparticles from the enclosing matrix the outer layer of ZrO_2 :20%PbS film was etched with Ar^+ ions. It was found experimentally that the film is fully removed from the glass substrate after 360 s of the etching. By using the measured thickness of the film the etching rate $330/6 = 55 \text{ nm/min}$ was found. Etching of ZrO_2 and PbS materials takes place at different rates, therefore locations of PbS nanoparticles are revealed in ZrO_2 :20%PbS film which look like pores. By analysing the diameters and mutual alignment of the pores it is possible to determine the diameters and mutual alignment of the nanoparticles in a single plane.

SEM images of ZrO_2 :PbS film taken at different magnifications are shown in Fig. 3.2. Location sites of PbS nanoparticles are seen as dark pores. The images demonstrate that the nanoparticles are mutually separated and do not form agglomerates.



3.2. att. SEM images of ZrO_2 :20%PbS film surface after 5 min of ion etching taken at different magnifications:

(a) 500 nm scale; (b) 50 nm scale

In order to estimate the diameters and distribution of diameters of PbS nanoparticles, SEM image seen in Fig.3.2(b) was processed with *ImageJ* software. The number of nanoparticles and the cross-sectional area of each nanoparticle were obtained. By approximating the shape of the nanoparticles as a circle, its diameter can be calculated:

$$d = 2 \cdot \sqrt{\frac{S}{3,14}} \quad (3.7)$$

where d – diameter of the nanoparticles, nm;
 S – cross-sectional area of the nanoparticles, nm².

The histogram of nanoparticle diameter distribution was obtained using *Ms Excel Data Analysis/Histogram* tool (Fig. 3.3).

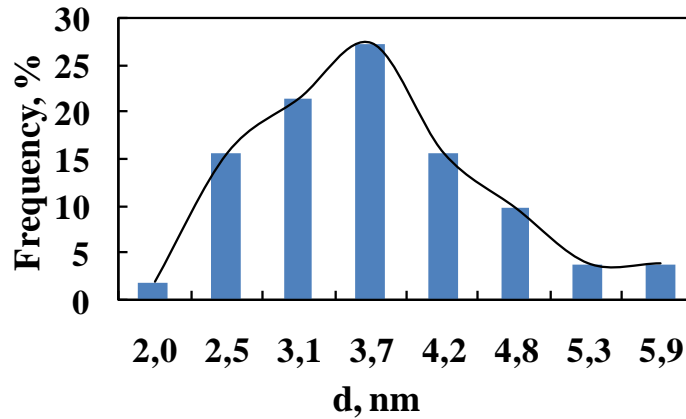


Fig. 3.3. The histogram of PbS nanoparticle diameter distribution in ZrO₂:20%PbS film

It should be taken into consideration that the etching process might result in expansion of nanoparticle location sites, therefore the diameters of nanoparticles obtained with SEM were compared to data available in the literature for the nanoparticles synthesized using the same technique. In references [40, 42, 43, 44] the diameters of the nanoparticles were obtained using TEM (transmission electron microscopy) and optical absorption measurements. In these references the diameters of PbS nanoparticles in ZrO₂:PbS film fabricated with 20% mole percent of PbS and annealed at 200 °C after deposition on the glass substrate were in a range of 2,5–4,5 nm. The measurements taken using SEM technique show that the diameters of PbS nanoparticles (exceeding 5% frequency) are in a range of 2,5–4,8 nm which corresponds to the data available in the literature. It can be concluded that SEM technique can be used for determination of diameters and mutual alignment of the nanoparticles. TEM technique cannot be applied for the given samples on the glass substrate because the thickness of the sample does not allow electrons to pass through the layers of the film and its substrate.

3.3. General processing of photoelectron emission spectra

Dependence of a number of electrons emitted per unit time I (el/s) on a wavelength λ (nm) of UV light exciting the emission is obtained while registering PE current. Energy E of light in electronvolts (eV) [3]:

$$E = 1240 / \lambda \quad (3.8)$$

PE current is proportional to the intensity of electromagnetic radiation (Stoletov's law) [3], therefore, it is necessary to take into account the different relative intensity of *DDS-30* lamp at different wavelengths. Magnitude of the registered emission current I was corrected using Equation (3.9) in order to account for relative intensity of the UV source at different wavelengths:

$$N = I \cdot \frac{98}{-0,0000014222 \cdot \lambda^4 + 0,0017035071 \cdot \lambda^3 - 0,7547089233 \cdot \lambda^2 + 145,8426442567 \cdot \lambda - 10268,4967892118}, \quad (3.9)$$

where N – corrected value of PE current, el/s.

PE current was measured from 3 randomly selected points on the sample surface and the arithmetic mean of the values measured for each photon energy was calculated.

The relative standard error of the mean of PE current measurements denoted by S_N (%) was estimated [4]:

$$S_N (\%) = \frac{S_N}{N} \cdot 100\% \quad (3.10)$$

where N – the arithmetic mean of PE current measurements, el/s;

S_N – the standard error of the mean of PE current measurements, el/s.

The standard error of the mean of PE current measurements [4]:

$$S_N = \frac{S}{\sqrt{n}}, \quad (3.11)$$

where $n=3$ – the number of measurements;

S – the standard deviation of PE current measurements, el/s.

The standard deviation of PE current measurements [4]:

$$S = \sqrt{\frac{\sum N_i^2 - \frac{\left(\sum_{i=1}^n N_i\right)^2}{n}}{n-1}}, \quad (3.12)$$

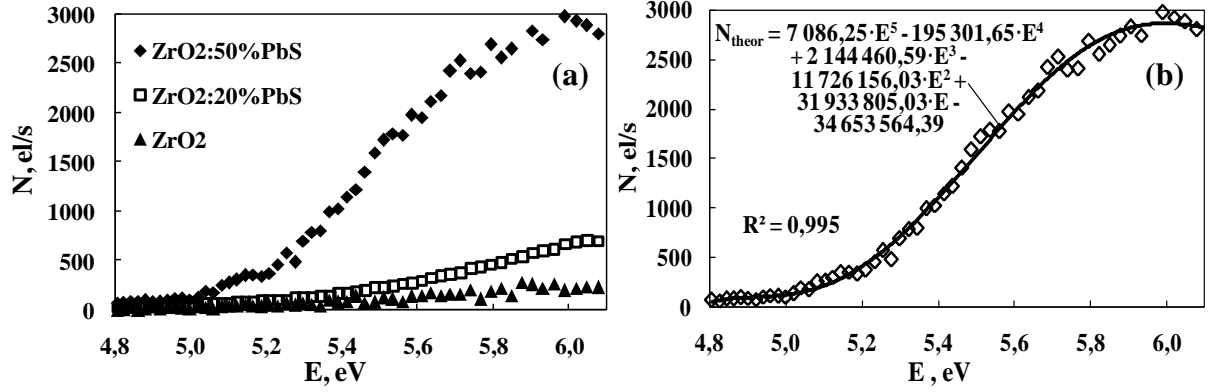
where N_i – PE current measured from a single point on the sample surface, el/s.

The relative standard error of the mean of PE current did not exceed 15% in energy range of PE exciting photons above 4,8 eV.

3.4. Influence of PbS nanoparticles on photoelectron emission of ZrO₂:PbS nanostructured films

In order to extract PE signal associated with the presence of PbS nanoparticles out of PE spectra of ZrO₂:PbS film, PE spectra of ZrO₂, ZrO₂:20%PbS and ZrO₂:50%PbS materials were compared (Fig. 3.4.(a)). PE intensity increases with increase in concentration of PbS nanoparticles. PE was also observed for ZrO₂ film despite the fact that photoelectron work function from ZrO₂ material exceeds photon energy used to excite PE (2.2.1. Chapter). Perhaps registered PE is associated with defects inherent in the structure of ZrO₂ [16].

To simplify further calculations, PE spectra were approximated with a fifth-degree polynomial using *MS Excel Trendline* function (coefficient of determination was $R^2=0,99$). The approximation results in smoothing of PE spectrum and fine components of the spectrum are inevitably lost, however, the basic shape of spectrum remains which can be used to analyze the behaviour of the spectrum in a wide energy range. As an example, the fifth-degree polynomial approximation of PE spectra of non-irradiated ZrO₂:50%PbS film is shown in Fig. 3.4.(b).



3.4. att. PE spectra of the films:
 (a) ZrO_2 , $ZrO_2:20\%PbS$ and $ZrO_2:50\%PbS$ films; (b) approximation of PE spectrum of $ZrO_2:50\%PbS$ film with the fifth-order polynomial

The mean error of polynomial approximation A did not exceed 10% for all experiments. It was calculated as [4]:

$$A = \frac{1}{n} \cdot \frac{\sum_{i=1}^n |N_i - N_{theor,i}|}{N_i} \cdot 100\% \quad (3.13)$$

where N_i – value of PE current measured in the experiment at energy E_i , el/s;
 $N_{theor,i}$ – value of PE current calculated from the equation of polynomial approximation by putting into it the corresponding E_i value, el/s;
 n – number of approximated data points.

Using Equation (3.14) of the polynomial approximation, first-order derivatives of PE spectra were calculated (Equation (3.15)). The constants of the polynomial equation were calculated using *Ms Excel LINEST* function. First-order derivatives of PE spectra describe concentration of active PE centres [10].

$$N = a \cdot E^5 + b \cdot E^4 + c \cdot E^3 + d \cdot E^2 + e \cdot E + f \quad (3.14)$$

$$dN/dE = 5 \cdot a \cdot E^4 + 4 \cdot b \cdot E^3 + 3 \cdot c \cdot E^2 + 2 \cdot d \cdot E + e \quad (3.15)$$

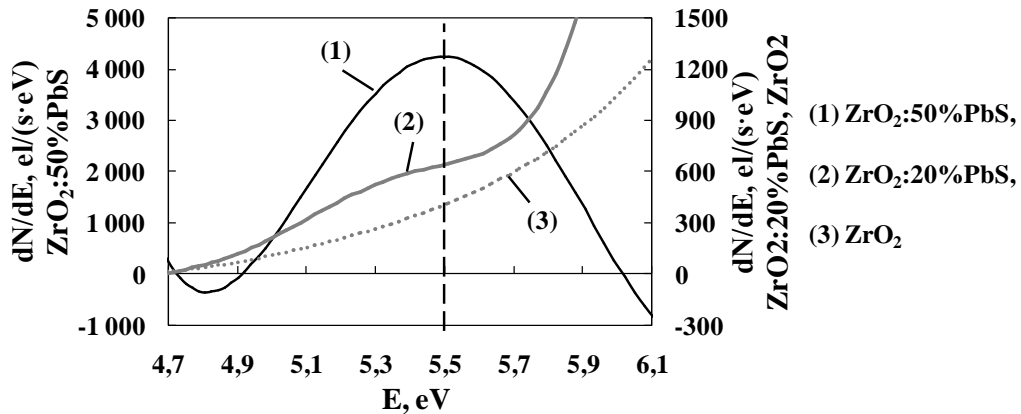


Fig. 3.5. Derivatives of PE spectra of $ZrO_2:50\%PbS$, $ZrO_2:20\%PbS$ and ZrO_2 films

In order to evaluate influence of PbS nanoparticles on the formation of active PE centres, derivatives of PE spectra of $ZrO_2:50\%PbS$, $ZrO_2:20\%PbS$ and ZrO_2 films were compared (Fig. 3.5). Derivative of PE spectra of $ZrO_2:50\%PbS$ film has a maximum at 5,5 eV, its width is 4,9–6,0 eV. This indicates that the highest concentration of PE active

centres in the film is at 5,5 eV. Derivative of PE spectra of ZrO₂:20%PbS film has an inflection point at 5,5 eV which means that the film has active PE centres at 5,5 eV, however the concentration of these centres is smaller than in ZrO₂:50%PbS film which has the distinct maximum at 5,5 eV. The maximum at 5,5 eV is not observed in case of ZrO₂ film which gives evidence that PE centres at 5,5 eV exist due to the presence of PbS nanoparticles in the film.

It is possible to conclude from Fig 3.5 that PbS nanoparticles provide different shape of derivative than ZrO₂ film, changes in concentration of PbS influence height of derivative graph, and in order to extract PE signal associated with PbS nanoparticles out of PE spectra of ZrO₂:PbS films, PE spectra in energy range of 4,9–6,0 eV must be analyzed.

The area below the derivative of PE spectra calculated in energy range from E_1 to E_2 is directly proportional to the number of electrons emitted within this range [10] and equals to the increment of PE current in energy range from E_1 to E_2 (Fig. 3.6):

$$\int_{E_1}^{E_2} \frac{dN}{dE} dE = N_2 - N_1 = \delta N \quad (3.16)$$

The standard error of PE current N_i is $\pm S_{Ni}$ (Equation (3.11)). By using PE spectra approximated with the fifth-degree polynomial, energy range from $(E_i - \Delta E_i)$ to $(E_i + \Delta E_i')$ was found that corresponded to the values of PE current from $(N_i - S_{Ni})$ to $(N_i + S_{Ni})$, and the arithmetic mean \bar{N}_i was calculated from PE data points that were experimentally measured within this energy range. Increment δN of PE current was calculated as difference between values of \bar{N}_2 and \bar{N}_1 :

$$\delta N = \bar{N}_2 - \bar{N}_1 = \frac{\sum_{i=1}^n N_i \Big|_{E_2 - \Delta E_2}^{E_2 + \Delta E_2'}}{n} - \frac{\sum_{i=1}^m N_i \Big|_{E_1 - \Delta E_1}^{E_1 + \Delta E_1'}}{m} \quad (3.17)$$

where n – number of PE measurement points in energy range from $(E_2 - \Delta E_2)$ to $(E_2 + \Delta E_2')$;
 m – number of PE measurement points in energy range from $(E_1 - \Delta E_1)$ to $(E_1 + \Delta E_1')$.

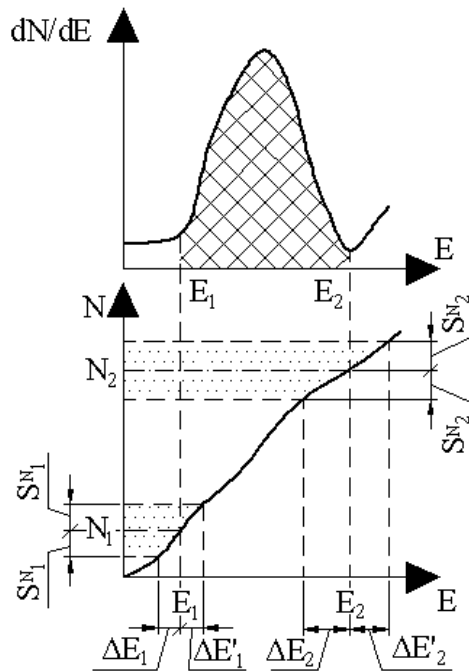


Fig. 3.6. The area below the derivative of PE spectra calculated in energy range from E_1 to E_2 equals to the increment of PE current in energy range from E_1 to E_2

It is possible that the maximum of derivative of PE current is formed by the superposition of several active PE centres whose quantity and position on the energy axis is not known (Fig. 3.7). For nanodosimetry applications it is important to extract only those centres that provide the largest PE signal of PbS nanoparticles. To test the hypothesis that some of the emission centres provide larger signal of PbS nanoparticles than the others, the maximum seen in Fig.3.5 was divided into half-widths in energy ranges of 4,9–5,5 eV and 5,5–6,0 eV, and influence of radiation on the each half-width was analyzed separately. The full-width 4,9–6,0 eV of the maximum was also analysed as a comparison.

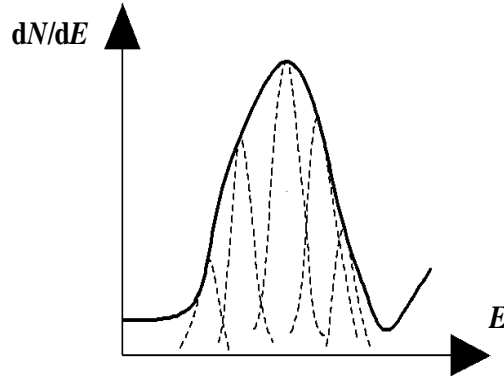


Fig. 3.7. Formation of the maximum of derivatives of PE spectra from superposition of some smaller maximums

The value of δN (Equation 3.17) was calculated for the each energy range and δN between $ZrO_2:PbS$ films with 20% and 50% mole rate of PbS were compared (Fig. 3.8).

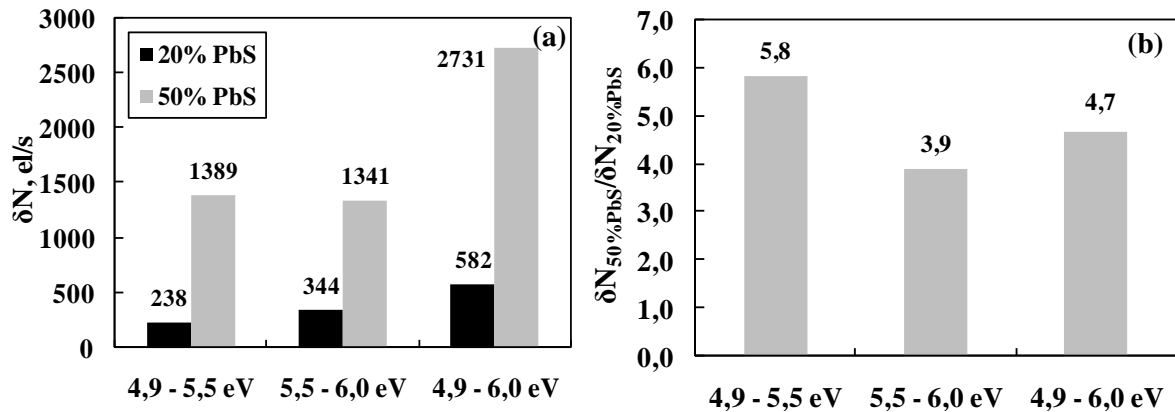


Fig. 3.8. Increments of PE current for $ZrO_2:PbS$ films with 20% and 50% mole rate of PbS calculated for different energy ranges:

(a) absolute values; (b) ratio between increments of PE current for films with 50% and 20% mole percent of PbS

Fig. 3.8 demonstrates that concentration of PbS nanoparticles has the greatest influence on the increment of PE current in energy range of 4,9–5,5 eV, since this range has the highest δN ratio between the films with 50% and 20% mole percent of PbS ($\delta N_{50\%PbS} / \delta N_{20\%PbS} = 1389/238 = 5,8$). This gives evidence that it is precisely the energy range from 4,9–5,5 eV for PbS nanoparticles provide the largest PE signal.

3.5. Influence of radiation on photoelectron emission of $\text{ZrO}_2\text{:PbS}$ nanostructured films

3.5.1. Influence of non-ionizing ultraviolet radiation on photoelectron emission of $\text{ZrO}_2\text{:PbS}$ nanostructured films

PE intensity from $\text{ZrO}_2\text{:PbS}$ films decreases with increase in time of UV exposure. As an example, PE spectra of the films with the highest mole percent of PbS (50%) are shown (Fig. 3.9).

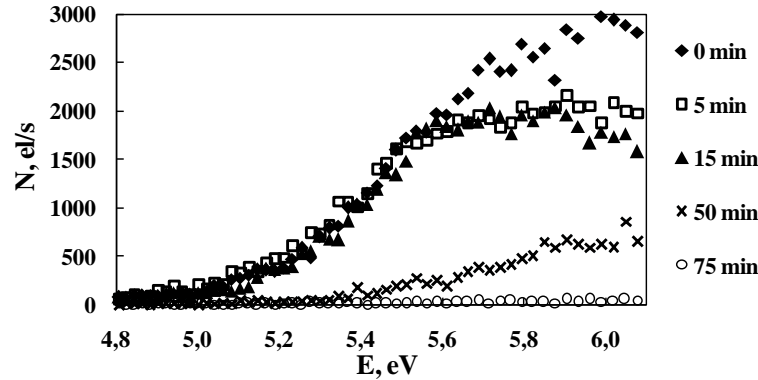


Fig. 3.9. PE spectra of $\text{ZrO}_2\text{:50%PbS}$ films after different time of UV exposure

In order to examine whether absorption of radiation has different effect on ZrO_2 matrix and PbS nanoparticles, PE spectra of irradiated $\text{ZrO}_2\text{:50%PbS}$ and $\text{ZrO}_2\text{:20%PbS}$ films were compared to PE spectra of irradiated ZrO_2 film. Using Equations (3.13) and (3.14) derivatives of PE spectra of $\text{ZrO}_2\text{:50%PbS}$, $\text{ZrO}_2\text{:20%PbS}$ and ZrO_2 films were calculated.

In order to evaluate the influence of UV radiation on ZrO_2 matrix and PbS nanoparticles, derivatives of PE spectra of non-irradiated and 50 minutes with UV irradiated $\text{ZrO}_2\text{:50%PbS}$ and ZrO_2 films were compared (Fig. 3.10 (a) and (b)). The derivative maximum of $\text{ZrO}_2\text{:50%PbS}$ films at 5,5 eV disappears after UV irradiation, this means that UV light decreases concentration of active PE centres. ZrO_2 films respond to UV light in the opposite way – concentration of active PE centres in ZrO_2 increases after UV irradiation (shown by the height of dN/dE graph).

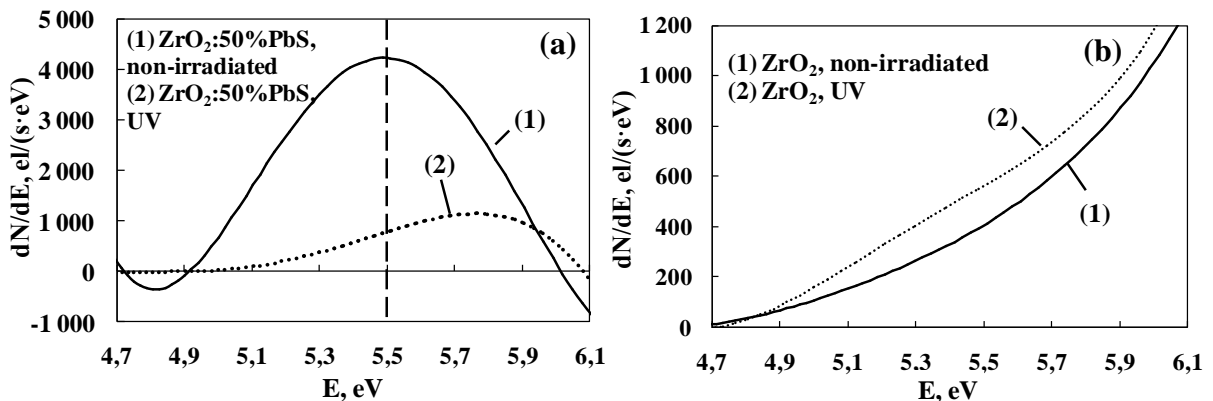


Fig. 3.10. Derivatives of PE spectra of non-irradiated and 50 minutes UV-irradiated films: (a) $\text{ZrO}_2\text{:50%PbS}$ film; (b) ZrO_2 film

Derivative of PE spectra of $\text{ZrO}_2\text{:20%PbS}$ film before and after 50 minutes of UV irradiation is seen in Fig. 3.11. Concentration of active PE centres in $\text{ZrO}_2\text{:20%PbS}$ film, similarly as in $\text{ZrO}_2\text{:50%PbS}$ film, decreases after UV irradiation.

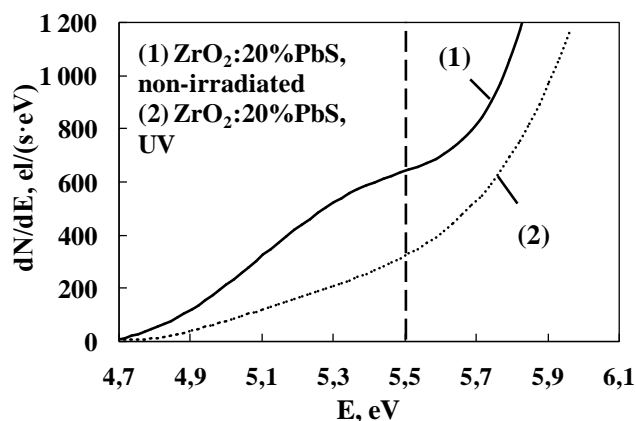


Fig. 3.11. Derivative of PE spectra of non-irradiated and 50 minutes with UV irradiated $\text{ZrO}_2\text{:}20\%\text{PbS}$ film

From Fig. 3.10 and 3.11 it was concluded that:

1) UV radiation has different effect on PbS nanoparticles and ZrO_2 material, therefore it is possible to extract PE signal of PbS nanoparticles out of PE spectra of $\text{ZrO}_2\text{:PbS}$ films that is influenced by absorption of radiation.

2) Absorption of radiation influences PE signal of PbS nanoparticles already at 20% mole percent of PbS in $\text{ZrO}_2\text{:PbS}$ film. This means that it is possible to continue research of $\text{ZrO}_2\text{:}20\%\text{PbS}$ films for nanodosimetry of ionizing radiation. (By contrast, it would not be possible to use $\text{ZrO}_2\text{:}50\%\text{PbS}$ films in nanodosimetry as PbS nanoparticles in these films are not mutually separated (unlike $\text{ZrO}_2\text{:}20\%\text{PbS}$ film – Fig.3.3)

3.5.2. Influence of ionizing electron beam radiation on photoelectron emission of $\text{ZrO}_2\text{:PbS}$ nanostructured films

$\text{ZrO}_2\text{:}20\%\text{PbS}$ films were exposed to electron beam radiation. ZrO_2 and $\text{ZrO}_2\text{:}50\%\text{PbS}$ films were no longer researched because these films cannot be used for nanodosimetry and experiments with non-ionizing UV radiation showed that PbS nanoparticles already provide PE signal at 20% mole percent of PbS.

In the experiments with ionizing radiation, each $\text{ZrO}_2\text{:}20\%\text{PbS}$ film was irradiated with its own dose of electrons, and PE spectra before and after irradiation were compared for each film. PE intensity decreases after irradiation with electron beam, as shown by the ratio of PE intensity after and before the irradiation ($N_{\text{Gy}}/N_0 < 1$) (Fig. 3.12).

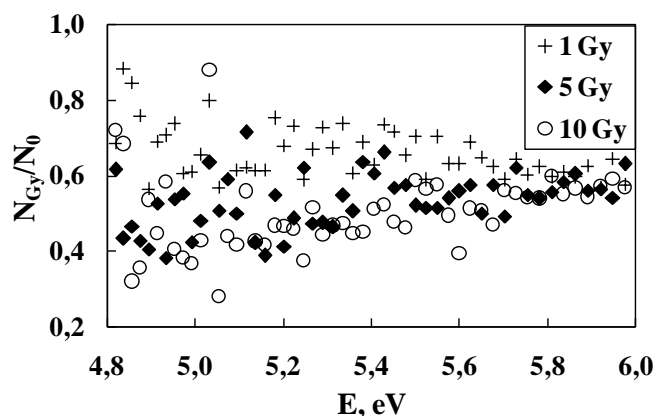


Fig. 3.12. Ratio of PE intensity of $\text{ZrO}_2\text{:PbS}$ films after and before the irradiation with electrons

As it was found previously, the greatest PE signal of PbS nanoparticles is provided within energy range of 4,9–5,5 eV (Fig. 3.8(b)). However, to verify that ionizing electron radiation has the greatest effect on the emission centres of PbS nanoparticles, two other energy ranges shown in Fig. 3.8(b) (5,5–6,0 eV and 4,9–6,0 eV) were also examined.

The increments of PE current before (δN_0) and after (δN_{Gy}) irradiation were calculated in energy ranges of 4,9–6,0 eV, 4,9–5,5 eV and 5,5–6,0 eV by using Equation (3.17). Change in increment of PE current after irradiation:

$$\Delta_{\delta N} = \delta N_{Gy} - \delta N_0 \quad (3.18)$$

For each energy range the relation between $\Delta_{\delta N}$ and the delivered dose of radiation D was derived. The experimental points were approximated with a theoretical curve $D_{theor}=f(\Delta_{\delta N})$. The best approximation between the experimental points and the theoretical curve is observed in the energy range of 4,9–5,5 eV which corresponds to PE signal of PbS nanoparticles (Fig. 3.12). This confirms the hypothesis that PbS nanoparticles can serve as sensitive elements of the nanodosimeter. For the energy range of 4,9–5,5 eV the relation between D_{theor} and $\Delta_{\delta N}$ is given by the second-degree polynomial:

$$D_{theor} = 2,168 \cdot 10^{-4} \cdot \Delta_{\delta N}^2 + 2,517 \cdot 10^{-2} \cdot \Delta_{\delta N} + 1,101 \quad (3.19)$$

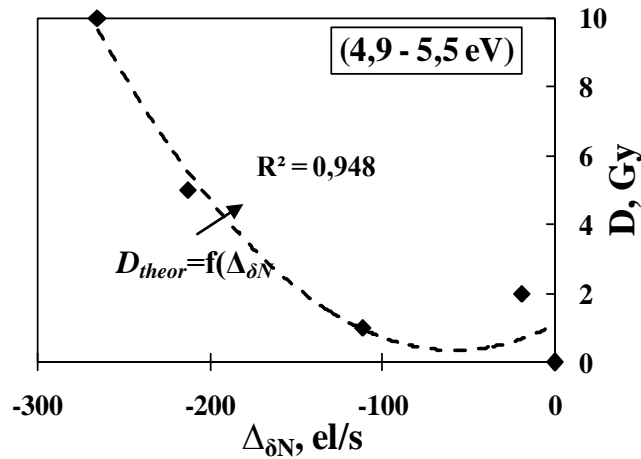


Fig. 4.9. Calibration curve describing relation between the change in increment of PE current of $ZrO_2:PbS$ films in energy range of 4,9–5,5 eV and absorbed dose of electron beam radiation

Formula (3.19) is the calibration equation of $ZrO_2:20\%PbS$ film nanodosimeter. By putting measured values of $\Delta_{\delta N}$ into this equation, it is possible to determine doses of ionizing radiation absorbed in the nanodosimeter.

3.5.3. Electron beam radiation dose measurement error

Theoretical dose $D_{theor,i}$ was calculated by putting the measured values of $\Delta_{\delta N}$ into Equation (3.19). Theoretical doses $D_{theor,i}$ were compared with the delivered doses D . Dose measurement error is defined as $\Delta D_i = |D_{theor,i} - D_i|$. Relative error of dose measurement is $\Delta D_i/D_i \cdot 100\%$ (Fig. 3.13).

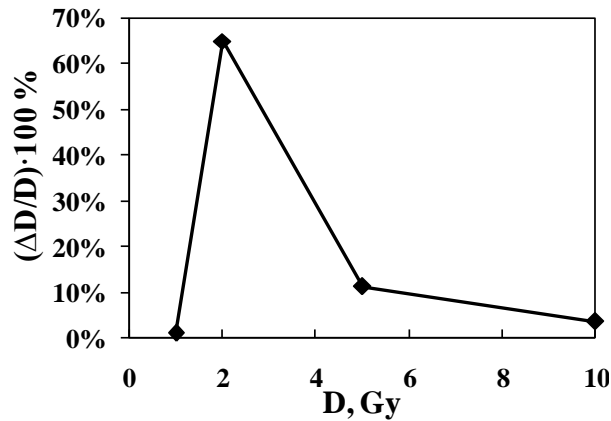


Fig. 3.13. Relative error of dose measurement depending on dose of electron beam radiation absorbed in $\text{ZrO}_2:20\%\text{PbS}$ films

Relative error of dose measurement decreases from 65% to 11% when the absorbed dose increases from 2 to 5 Gy. Relative error of dose measurement does not exceed 11% in dose range of 5–10 Gy.

3.6. Restoration of $\text{ZrO}_2:\text{PbS}$ nanostructured films after exposure to electron beam radiation

3.6.1. Selection of annealing temperature

Annealing of $\text{ZrO}_2:20\%\text{PbS}$ films irradiated with electrons must be performed at highest possible temperature in order to effectively restore active FE centres to their pre-irradiation condition. However, the temperature must not be too high to avoid damage of the films.

In order to determine the maximum annealing temperature that does not damage the films, the non-irradiated films were annealed. PE from the films was measured before and after annealing. If the annealing temperature does not damage the film, PE intensity must also remain constant after annealing.

$\text{ZrO}_2:20\%\text{PbS}$ films were annealed at 200 °C for 30 minutes during the fabrication (2.2.1 Chapter), therefore, similar annealing temperatures 200 °C and 250 °C were first tested. Condition of the films after annealing was controlled both visually and by registering PE spectra. The surface of $\text{ZrO}_2:20\%\text{PbS}$ films turned brown after annealing (Fig. 3.14(a)). To verify that the color change results from damage to the film rather than from other uncontrollable factors, the glass substrate was annealed under identical conditions. The glass surface did not change visually after annealing (Fig. 3.14(b)), indicating that the changes in $\text{ZrO}_2:\text{PbS}$ film resulted from inappropriate annealing temperatures.

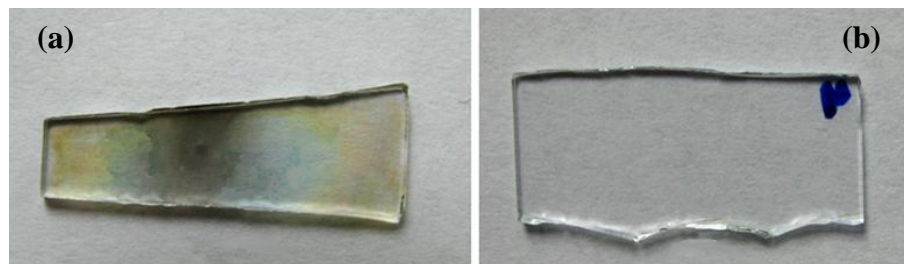
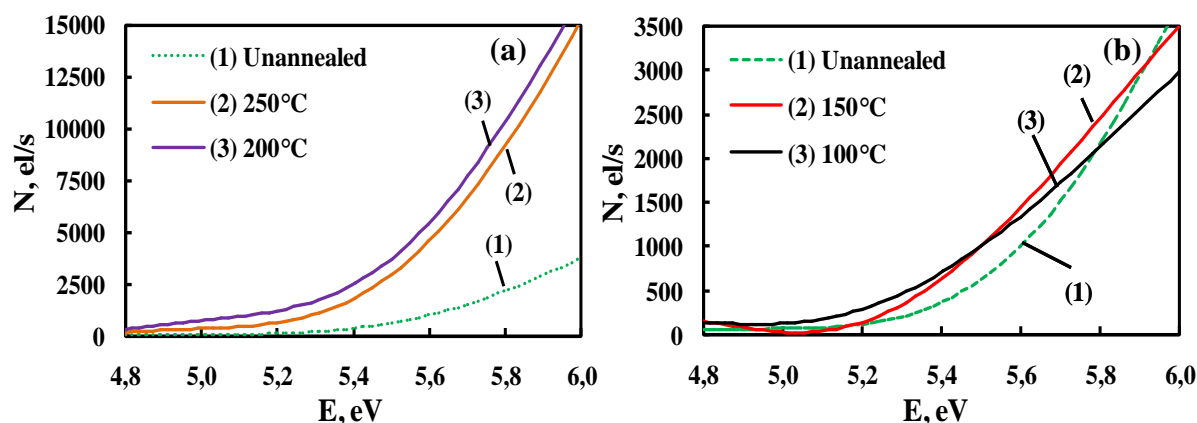


Fig. 3.14. Visual appearance of the samples annealed at 250 °C for 30 minutes (a) $\text{ZrO}_2:20\%\text{PbS}$ film; (b) glass substrate

PE measurements also demonstrate that ZrO₂:20%PbS films were damaged. PE spectra of the films measured after 7 days after annealing are shown in Fig. 3.15(a). PE spectra were approximated with a fifth-degree polynomial using *MS Excel Trendline* function (coefficient of determination $R^2=0,99$). PE current from the annealed films was 5 times higher than PE current from the unannealed films, proving that the films were damaged during annealing and this damage was significant, because PE spectra of the annealed films were different from PE spectrum of the unannealed film even after 7 days.



3.15. att. PE spectra of ZrO₂:20%PbS films annealed at different temperatures (a) at 200 °C un 250 °C for 30 minutes; (b) at 100 °C un 150 °C for 30 minutes

Lower annealing temperatures 100 °C and 150 °C were tested next. By visual observation of ZrO₂:PbS films it was found that annealing at 150 °C did not change the color of the films. PE measurements also prove that annealing at 100 °C and 150 °C does not damage the surface of the films because PE spectra of the annealed and unannealed films coincide (shown after 7 days after annealing) (Fig. 3.15(b)). For further experiments annealing temperature 150 °C was chosen as optimal.

3.6.2. Time-dependent changes of photoemission spectra after annealing

In order to examine influence of annealing on stability of PE from ZrO₂:20%PbS films, the following experiments were performed:

- PE measurements from the non-irradiated ZrO₂:20%PbS films.
- Irradiation of the films with 10 Gy dose of electrons.
- PE measurements from the irradiated films.
- Annealing of the irradiated films at 150 °C during 30 minutes and cooling at a natural rate to room temperature.
- PE measurements from the annealed films.

PE intensity from ZrO₂:20%PbS film irradiated with 10 Gy of electrons decreases (Fig. 3.16(a) – (2)) in comparison with PE intensity from non-irradiated film (1). PE intensity from the irradiated and annealed film measured on the next day after annealing (3) is 5 times higher than PE intensity from the non-irradiated film (1). In the following days, PE intensity decreases and approaches PE intensity from the non-irradiated films ((4) and (5)). On Day 4 after annealing, PE intensity from the irradiated film (6) coincides with PE intensity from the non-irradiated film (1) – the film has returned to its pre-irradiation condition.

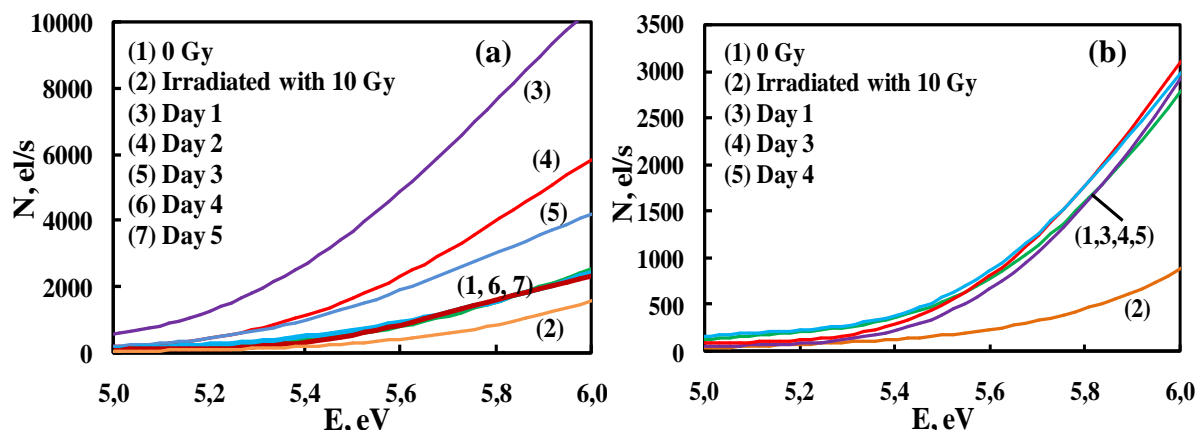


Fig. 3.16. PE spectra of irradiated films registered at different times after annealing: (a) $ZrO_2:PbS$ film; (b) ZrO_2 film

Analyzing PE spectra in Fig. 3.16(a), it was concluded that $ZrO_2:20\%PbS$ film returns to its pre-irradiation condition after 4 days after annealing and it is possible to irradiate $ZrO_2:20\%PbS$ films with ionizing radiation again no earlier than on Day 4 after annealing.

For comparison, ZrO_2 film was irradiated with the dose of 10 Gy and annealed (Fig. 3.16(b)). PE intensity from the annealed ZrO_2 film coincided with PE from the non-irradiated film (1) already on the next day after annealing (3) and did not change in the following days ((4) and (5)). This proves that return of PE intensity from $ZrO_2:20\%PbS$ films to the pre-irradiation condition during 4 days after annealing is related to the presence of PbS nanoparticles.

3.6.3. Exposure of $ZrO_2:PbS$ nanostructured films to electron beam radiation after annealing

The possibility to irradiate the annealed $ZrO_2:20\%PbS$ films and use them again for dosimetry was examined. The non-irradiated films were irradiated with 10 Gy dose of electrons, annealed, and irradiated with 10 Gy again on Day 4 after annealing (Fig. 3.18).

PE intensity decreases after the first irradiation (2) in comparison with PE intensity of non-irradiated film (1). PE spectrum was registered on Day 4 after annealing (3) and it was found that PE intensity coincided with the pre-irradiation PE intensity (1). After repeated irradiation of the film with 10 Gy of electrons, PE intensity decreased again (4) and coincided with PE intensity recorded after the first irradiation (2).

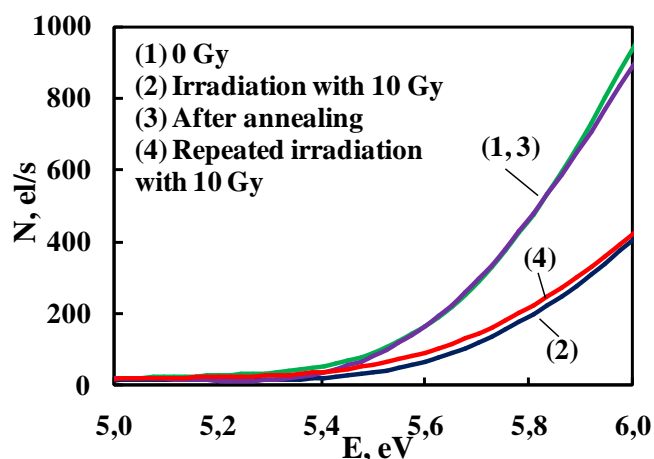


Fig. 3.18. Influence of repeated irradiation on PE spectra of annealed $ZrO_2:20\%PbS$ film

In order to determine whether PE intensity recovery effect remains after multiple cycles of irradiation and annealing, $\text{ZrO}_2:20\%\text{PbS}$ film was irradiated multiple times with 10 Gy of electrons, each time annealing of the film was performed before the irradiation. PE spectra were recorded after each irradiation and annealing (Fig. 3.19). It was found that PE intensity recovery effect remains.

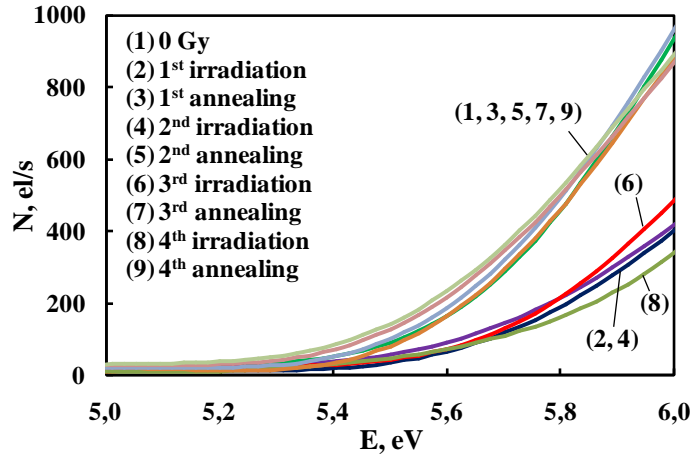


Fig. 3.19. PE intensity recovery effect for $\text{ZrO}_2:20\%\text{PbS}$ film after multiple cycles of irradiation and annealing

Recovery of PE intensity after multiple cycles of irradiation and annealing evidence that it is possible to restore the nanodosimeter made of $\text{ZrO}_2:20\%\text{PbS}$ film to its pre-irradiation condition multiple times.

CONCLUSIONS

1) Nanodosimetry is possible if the active elements of a nanodosimeter are made of semiconductor nanoparticles with high absorption coefficient of radiation and a diameter comparable to the diameter of the DNA (few nanometers). The nanoparticles must be embedded into a dielectric matrix that provides physical and chemical stability of the nanoparticles. The nanoparticles together with the dielectric matrix form a nanostructured film.

2) It has been demonstrated for the first time that ZrO₂ films with embedded PbS nanoparticles (ZrO₂:PbS nanostructured films) can be used for nanodosimetry of ionizing radiation. Dose readout is provided by measurements of photoelectron emission from PbS nanoparticles.

3) PbS nanoparticles create photoemission active centres in ZrO₂:PbS nanostructured film. In order to excite photoelectron emission from the active centres created by PbS nanoparticles, photons in energy range of 4,9–5,5 eV have to be used. Concentration of the active photoemission centres decreases under influence of ionizing radiation.

4) The method of dosimetry of ionizing radiation based on photoelectron emission from ZrO₂:PbS nanostructured films has been developed which allows to measure dose of ionizing radiation absorbed in a nanoobject. The calibration curve has been obtained which allows to measure dose of 9 MeV electron beam radiation absorbed in ZrO₂:PbS nanostructured films in dose range of 0–10 Gy. Error of absorbed dose measurement decreases from 65% to 11% when the dose increases from 2 to 5 Gy and does not exceed 11% in dose range of 5–10 Gy.

5) The method of annealing of ZrO₂:PbS nanostructured films has been developed which allows to erase dose of ionizing radiation stored in the films. It has been demonstrated that annealing of the films in vacuum at 150 °C for 30 minutes erases dose of ionizing radiation absorbed in the films and restores the photoelectron emission of the film to the initial pre-irradiation condition. Restoration of the films to the pre-irradiation condition takes place during 4 days after annealing; therefore the repeated irradiation of the films is possible not earlier than after 4 days after annealing. PE recovery effect persists after multiple cycles of irradiation and annealing.

RECOMMENDATIONS

In order to promote use of ZrO₂:PbS nanostructured films and method of photoemission in nanodosimetry, the following is suggested:

1) It is necessary to improve method of dose reading in order to reduce dose reading error to 1% especially for doses less than 2 Gy.

2) Further metrological studies are necessary to assess influence of external conditions (humidity, temperature) on long-term storage of the absorbed dose in a nanodosimeter.

3) Exposure of ZrO₂:PbS nanostructured films to different types, energies and doses of ionizing radiation is required in order to define range of use and possibilities of ZrO₂:PbS nanodosimeter.

4) To make calibration of the nanodosimeter based on the radiation-induced changes in the DNA molecule.

LIST OF LITERATURE

1. Akmene R.J., Balodis A.J., Dekhtyar Yu. D., Markelova G.N., Matvejevs J.V., Rozenfelds L.B., Sagalovich G.L., Smirnovs J.S., Tolkachovs A.A., Upmiņš A.I. Exoelectron emission spectrometre complete set of surface local investigation// *Surface: Physics, Chemistry, Mechanics*. - 1993. - Vol.8. - pp.125-128.
2. Alivisatos A.P. *Semiconductor Clusters, Nanocrystals, and Quantum Dots*// *Science, New Series*. - 1996. - Vol.271. - pp.933-937.
3. Apinis, A. *Fizika*.- Rīga: Zvaigzne, 1972. - 707.lpp.
4. Arhipova I., Bāliņa S. *Statistika ekonomikā. Risinājumi ar SPSS un Microsoft Excel*. - Rīga: Datorzinību centrs, 2003. - 352 lpp.
5. Bantsar A., Pietrzak M., Jaskóła M., Korman A., Pszona S., Szepliński Z. *Status report: Nanodosimetry of carbon ion beam at HIL*// *Reports of Practical Oncology and Radiotherapy*. - 2014. - Vol.19 - pp.S42-S46.
6. Baskar R., Lee KA, Yeo R, Yeoh KW. *Cancer and Radiation Therapy: Current Advances and Future Directions*// *International Journal on Medical Sciences*, Vol. 9, No. 3, 2012; 193-199.p.
7. Beddar A.S, Krishnan S. *Intraoperative radiotherapy using a mobile electron LINAC: A retroperitoneal sarcoma case*// *Journal of Applied Clinical Medical Physics*. - 2005. - Vol.6. - pp.95-107.
8. Beecroft L.L., Ober C.K. *Advanced Nanocomposite Materials for Optical Applications*// *Chemistry of Materials*. - 1997. - Vol.9. - pp.1302-1317.
9. Berkner L.V., Marshall L.C. *On the Origin and Rise of Oxygen Concentration in the Earth's Atmosphere*// *Journal of the Atmospheric Sciences*. - 1965. - Vol.22. - pp.225-261.
10. Carlson T.A. *Photoelectron and Auger Spectroscopy*. - New York: Plenum Press, 1975. - 417 p.
11. Clinac 2100C/D Varian, *Tehniskie raksturojumi/ Internet*.- <http://ru.medwow.com/med/linear-accelerator/varian/clinac-2100cd/35317.model-spec> [viewed 11.01.2015]
12. Conte V., De Nardo L., Colautti P., Ferretti A., Grosswendt B., Lombardi M., Poggi M., Canella S., Moro D., Tornielli G. *First track-structure measurements of 20 MeV protons with the STARTRACK apparatus*// *Radiation Measurements*. - 2010. - Vol.45. - pp.1213-1216.
13. Conte V., Grosswendt B., Colautti P., Moro D., De Nardo L. *Track-structure investigations: A supplement to microdosimetry*// *AIP Conference Proceedings*. - 2013. - Vol.1530. - pp.140-147.
14. Dehtjars J., Emziņš Dz., Jurkevičs A., Milano F. *un citi. Radiācijas drošība radiologu asistentiem*.- Rīga: RTU, 2006. - 336 lpp.
15. Dekhtyar Yu. *Emission of weak elections: Dosimetry of nanovolumes*// *Radiation Measurements*. - 2013. - Vol.55. - pp.34-37.
16. Emeline A., Kataeva G.V., Litke A.S., Rudakova A.V., Ryabchuk V.K., Serpone N. *Spectroscopic and Photoluminescence Studies of a Wide Band Gap Insulating Material: Powdered and Colloidal ZrO2 Sols*// *Langmuir*. - 1998. - Vol.14. - pp.5011-5022.
17. Fuks E., Horowitz Y.S., Horowitz A., Oster L., Marino S., Rainer M., Rosenfeld A., Datz H. *Thermoluminescence solid-state nanodosimetry-the peak 5a/5 dosemeter*// *Radiation Protection Dosimetry*. - 2011. - Vol.143. - 416-426.p.
18. Furetta C. *Handbook of Thermoluminescence*. - Singapore: World Scientific Publishing Co., 2003. - 446 p.
19. Garty G., Shchemelinina S., Breskina A., Chechika R., Assaf G., Orio I., Bashkirov V., Schulte R., Grosswendt B. *The performance of a novel ion-counting nanodosimeter*// *Nuclear Instruments and Methods in Physics Research A*. - 2002. - Vol.492. - pp.212-235
20. Gatan Inc. *Precision Etching Coating System, Model 682 / Internets*. - [http://www.glteam.com/pdf/682PECS\(New\).pdf](http://www.glteam.com/pdf/682PECS(New).pdf) [viewed 16.05.2015]
21. Grosswendt B. *Recent Advances of Nanodosimetry*// *Radiation Protection Dosimetry*. - 2004. - Vol.110. - pp.789-799.
22. Hall E.J., Giaccia A.J. *Radiobiology For The Radiologist*. - Philadelphia: Lippincott Williams & Wilkins, 2006. - 586 p.
23. HeatWave Labs *Model 101303-23 Temperature Controller, User's Manual / Internets*. - <http://www.cathode.com/pdf/HW101303-23Manual.pdf> [viewed 11.01.2015]
24. Hitachi S-4800 *Field Emission Scanning Electron Microscope / Internets*. - http://cmrf.research.uiowa.edu/files/cmrf.research.uiowa.edu/files/S-4800%20Instruction%20Manual_1.pdf [viewed 16.05.2015]
25. Hyun B.-R., Zhong Y.-W., Bartnik A.C., Sun L., Abruña H.D., Wise F.W., Goodreau J.D., Matthews J.R., Leslie T.M., Borrelli N.F. *Electron Injection from Colloidal PbS Quantum Dots into Titanium Dioxide Nanoparticles*// *ACS Nano*. - 2008. - Vol.2. - pp.2206-2212.
26. Ibach H. *Electron Spectroscopy for Surface Analysis*.- New York, SpringerVerlag, 1977. - 315.p
27. ICRU Report 85: *Fundamental Quantities and Units for Ionizing Radiation*// *Journal of the ICRU*. - 2011. - Vol.11. - pp.1-31.

28. Jordan L. Review of recent advances in non 3D dosimeters// *Journal of Physics: Conference Series*. - 2013. - Vol.444. - Article number 012009. - pp.1-8.
29. Konstantatos G., Sargent E.H. Nanostructured materials for photon detection// *Nature Nanotechnology*. - 2010. - Vol.5. - pp.391-400.
30. L8222 Radiant Spectrum Comparison / *Internets*. - <http://www.datasheetarchive.com/dl/Datasheet-028/DSA00487525.pdf> [viewed 11.01.2015]
31. Low D.A., Moran J.M., Dempsey J.F., Dong L., Oldham M. Dosimetry tools and techniques for IMRT// *Medical Physics*. - 2011. - Vol.38. - pp.1313-1338.
32. Ministru kabineta noteikumi Nr.149 no 09.04.2002. Noteikumi par aizsārdzību pret jonizējošo starojumu / *Internet*. - <http://likumi.lv/doc.php?id=61173> [viewed 27.12.2014]
33. Motic BA400 / *Internet*. - <http://www.meyerinst.com/html/motic/microscopes/B%20Series/BA400.pdf> [viewed 11.01.2015]
34. Nettelbeck H., Rabus H. Nanodosimetry: The missing link between radiobiology and radiation physics?// *Radiation Measurements*. - 2011. - pp.893-897.
35. Nieto J.A. Thermoluminescence Dosimetry (TLD) and its Application in Medical Physics// *AIP conference Proceedings*. - 2004. - Vol.724. - pp.20-27.
36. OECD, European Union. Health at a Glance: Europe 2014/ *Internet*. - http://ec.europa.eu/health/reports/european/health_glance_2014_en.htm [viewed 03.01.2015]
37. PCI Bus Compatible Counting Board M8784 / *Internet*. - <http://pdf.datasheetcatalog.com/datasheet/hamamatsu/M8784.pdf> [viewed 11.01.2015]
38. Photon and Electron Interactions With Matter / *Internet*. - <http://pdg.lbl.gov/1998/photonelecrpp.pdf> [viewed 18.01.2015]
39. Rabus H., Nettelbeck H. Nanodosimetry: Bridging the gap to radiation biophysics// *Radiation Measurements*. - 2011. - Vol.46. - 1522-1528.
40. Reisfeld R. Nanosized semiconductor particles in glasses prepared by the sol-gel method: their optical properties and potential uses// *Journal of Alloys and Compounds*. - 2002. - Vol.341. - pp.56-61.
41. Robertson J. Band offsets of wide-band-gap oxides and implications for future electronic devices// *Journal of Vacuum Science and Technology B: Microelectronics and Nanometer Structures*. - 2000. - Vol.18. - pp.1785-1791.
42. Saraidarov T., Reisfeld R., Sashchiuk A., Lifshitz E. NanoCrystallites of Lead Sulfide in Hybrid Films Prepared by Sol-Gel Process// *Journal of Sol-Gel Science and Technology*. - 2005. - Vol.34. - pp.137-145.
43. Sashchiuk A., Lifshitz E., Reisfeld R., Saraidarov T. Properties of PbS nanocrystals embedded in zirconia sol-gel films// *Materials Science and Engineering C*. - 2002. - Vol.19. - pp.67-71
44. Sashchiuk A., Lifshitz E., Reisfeld R., Saraidarov T., Zelnor M. Optical and Conductivity Properties of PbS Nanocrystals in Amorphous Zirconia Sol-Gel Films// *Journal of Sol-Gel Science and Technology*. - 2002. - Vol.24. - pp.31-38.
45. Seah M.P., Dench W.A. Quantitative electron spectroscopy of surfaces: A standard data base for electron inelastic mean free paths in solids// *Surface and Interface Analysis*. - 1979. - Vol.1. - pp.2-11.
46. Slimību profilakses un kontroles centrs: Veselības aprūpes statistika, Statistikas dati par 2013. gadu, Onkoloģija/ *Internet*. - <http://www.spkc.gov.lv/veselibas-aprupes-statistika/> [viewed 18.05.2015]
47. Slimību profilakses un kontroles centrs: Veselības aprūpes statistika, Statistikas dati par 2014.gadu, Mirstība/ *Internet*. - <http://www.spkc.gov.lv/veselibas-aprupes-statistika/> [viewed 18.05.2015]
48. Sors A., Cassol E., Latorzeff I., Duthil P., Sabatier J., Lotterie J.A., Redon A., Berry I., Franceries X. An optimized calibration method for surface measurements with MOSFETs in shaped-beam radiosurgery// *Physica Medica*. - 2014. - Vol.30. - pp.10-17.
49. Souris J.S., Cheng S.-H., Pelizzari C., Chen N.-T., La Riviere P., Chen C.-T., Lo L.-W. Radioluminescence characterization of in situ x-ray nanodosimeters: Potential real-time monitors and modulators of external beam radiation therapy// *Applied Physics Letters*. - 2014. - Vol.105. - Article number 203110. - pp.1-5.
50. Spectroscopy. Photonics Handbook / *Internet*. - <http://www.photonics.com/EDU/Handbook.aspx?AID=25118> [viewed 18.01.2015]
51. Spot light source LC8 LIGHTNINGCURE L8222 / *Internet*. - http://www.helmut-singer.de/pdf/hamamatsulc5_lc6.pdf [viewed 11.01.2015]
52. Standard Imaging, Inc. Micro Ion Chambers / *Internet*. - <http://www.standardimaging.com/exradin/micro-ion-chambers/> [viewed 01.01.2015]
53. The Geant4-DNA Project / *Internet*. - <http://geant4-dna.org/> [viewed 08.01.2015]
54. Ultraskaņas vanna „Bandelin Sonorex RK31”: Data Sheet / *Internet*. - http://bandelin.com/datenblaetter/RK/RK_31_H_BANDELIN.pdf [viewed 11.01.2015]
55. Добрецов Л.Н., Гомоюнова М.В. Эмиссионная электроника. - Москва: Наука, 1966. - 542 с
56. Лампа спектральная ДДС 30 (ЛД2-Д) / *Internet*. - http://www.medrk.ru/shop/index.php?id_group=71&id_subgroup=71&id_goods=10060 [viewed 11.01.2015]

57. Фоменко В.С. Эмиссионные свойства материалов.- Киев: Наукова думка, 1981. - 339 с
58. Энциклопедия физики и техники: Фотоэлектронная эмиссия / Internets. - http://www.femto.com.ua/articles/part_2/4392.html [viewed 22.01.2015]

ACKNOWLEDGEMENTS

I would like to express my gratitude to my doctoral supervisor Prof. Yuri Dekhtyar for guidance, advice, assistance in analysis of the obtained results and explanation of the physical nature of the observed effects.

I would like to thank Prof. Renata Reisfeld and researcher Tsiala Saraidarov from Hebrew University of Jerusalem for fabrication of the studied nanostructured films.

I also would like to thank medical physicist Indra Surkova for irradiation of the nanostructured films with ionizing radiation.

I am grateful to laboratory assistant Daniels Jevdokimovs for SEM measurements.

Thanks to all my colleagues from Institute of Biomedical Engineering and Nanotechnologies. Special thanks to Viktorija Vendiņa and Maksims Šneiders for editing corrections and critical remarks, to Prof. Alexei Katashev for consultations on processing of the results and to Vineta Zemīte for motivation and encouragement.

Thanks to my students Aļisa Rešetņikova and Pāvels Kovaļovs for enthusiasm and experimental acquisition of data.

I am also thankful to the secretary of “RTU P-16” Promotion Council Natālija Mozga for consultations on theses formatting and submitting issues.

Thanks to Department of doctoral studies of Riga Technical University.

A special thanks to my family for their support and motivation.